Structures Research Report No. 714 October, 2002
FINAL PROJECT REPORT

Contract Title: Post-Installed Reinforcing Bar Splices to Existing Reinforcement
UF Project No. 4910 4504 714 12
Contract No. BC354 RPWO #2

POST-INSTALLED ADHESIVE-BONDED SPLICES IN BRIDGE DECKS

Principal Investigator: Ronald A. Cook, Ph.D., P.E.

Graduate Research Assistant: Scott D. Beresheim

Project Manager: Marcus H. Ansley, P.E.

Department of Civil & Coastal Engineering
College of Engineering
University of Florida
Gainesville, Florida 32611

Engineering and Industrial Experiment Station

Technical Report Documentation Page

1. Report No.	2. Government Accession No.	3. Recipient's Catalog No.
BC354 RPWO #2		

4. Title and Subtitle	5. Report Date
Post-Installed Adhesive-Bonded Splices in Bridge Decks	October 2002
	6. Performing Organization Code
7. Author(s)	8. Performing Organization Report No.
R. A. Cook and S. D. Beresheim	4910 45 04 714
9. Performing Organization Name and Address	10. Work Unit No. (TRAIS)
University of Florida Department of Civil Engineering 345 Weil Hall / P.O. Box 116580 Gainesville, FL 32611-6580	11. Contract or Grant No. BC354 RPWO #2
12. Sponsoring Agency Name and Address	13. Type of Report and Period Covered Final Report
Florida Department of Transportation Research Management Center 605 Suwannee Street, MS 30 Tallahassee, FL 32301-8064	14. Sponsoring Agency Code

15. Supplementary Notes

Prepared in cooperation with the Federal Highway Administration

16. Abstract

The purpose of this study was to investigate the feasibility of using post-installed adhesive-bonded splices for bridge deck additions. Current bridge deck additions involve the removal of part of the existing bridge deck so that reinforcing bars for the new deck can be spliced with those in the existing deck. The alternative presented is to drill into the side of the existing deck and install reinforcing bars using a structural adhesive. The study includes both constructability concerns and structural requirements for the splices.

The specific objectives were to: examine the methods used to install adhesive splices and determine if the methods are practical for use on a job site; perform flexural tests to determine the splice length required to achieve full flexural strength when using an adhesive-bonded splice; perform shear tests to determine the shear strength of adhesive-bonded dowel bars; provide design recommendations for splice lengths for adhesive-bonded reinforcement in bridge decks additions; and provide design recommendations for determining the shear strength of adhesive-bonded dowel bars in bridge deck additions.

Four test series were performed to investigate the moment and shear capacity of post-installed adhesive-bonded reinforcement. Each test series consisted of a control specimen with no spliced reinforcement and four test specimens using adhesive-bonded splices with varied locations and embedment lengths. The results of these tests indicated that the splice length provisions of the ACI 318 and AASHTO codes are adequate and that the FDOT specifications for anchorage of adhesive-bonded anchors could be used with some modifications to account for splice length. For shear strength of adhesive-bonded dowel bars, the shear-friction provisions of ACI 318 and AASHTO are appropriate.

17. Key Words	18. Distribution Statement
Splice Length, Post-Installed Splices, Dowel Bars, Adhesive Anchors, Bridge Deck Additions	No restrictions. This document is available to the public through the National Technical Information Service, Springfield, VA, 22161

19. Security Classif. (of this report)	20. Security Classif. (of this page)	21. No. of Pages	22. Price
Unclassified	Unclassified	83	

Form DOT F 1700.7 (8-72)

DISCLAIMER

"The opinions, findings, and conclusions expressed in this publication are those of the authors and not necessarily those of the Florida Department of Transportation or the U.S. Department of Transportation.

Prepared in cooperation with the State of Florida Department of Transportation and the U.S. Department of Transportation."

POST-INSTALLED ADHESIVE-BONDED SPLICES IN BRIDGE DECKS

CONTRACT NO. BC 354 RPWO #2
UF NO. 4910 4504 714 12

PRINCIPAL INVESTIGATOR: RONALD A. COOK

GRADUATE RESEARCH ASSISTANT: SCOTT D. BERESHEIM

FDOT TECHNICAL COORDINATOR: MARCUS H. ANSLEY

ENGINEERING AND INDUSTRIAL EXPERIMENT STATION
DEPARTMENT OF CIVIL ENGINEERING
UNIVERSITY OF FLORIDA
GAINESVILLE, FLORIDA

TABLE OF CONTENTS

page

LIST OF TABLES

Table Page

LIST OF FIGURES

CHAPTER 1
INTRODUCTION

1.1 General

In the state of Florida, many bridges have larger volumes of traffic than they were initially designed to handle. Due to the greater traffic demand on these bridges, the Florida Department of Transportation (FDOT) is adding lanes to some of these bridges. Currently, to add a lane to an existing bridge, a portion of the bridge is removed, bars are spliced to the existing bars, and then the new bridge deck is cast. This method requires a large amount of time to remove part of the existing bridge deck. A possible alternative to the current method is the use of post-installed adhesive splices. This method involves drilling into the side of the existing bridge deck and installing reinforcing bars using a structural adhesive. This method eliminates the time and labor required for the partial removal of the bridge deck Figure 1.1 and Figure 1.2.

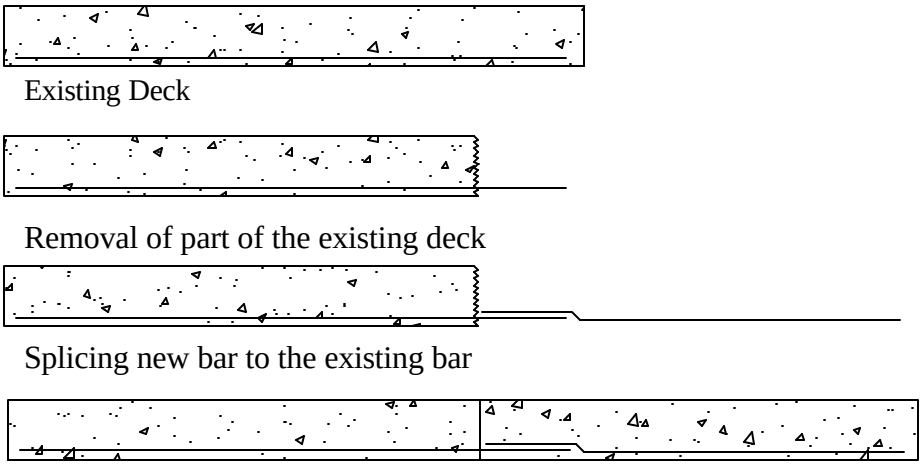

Existing Deck

Removal of part of the existing deck

Splicing new bar to the existing bar

Pouring the new deck

Figure 1.1 – Current method for installing splice bars.

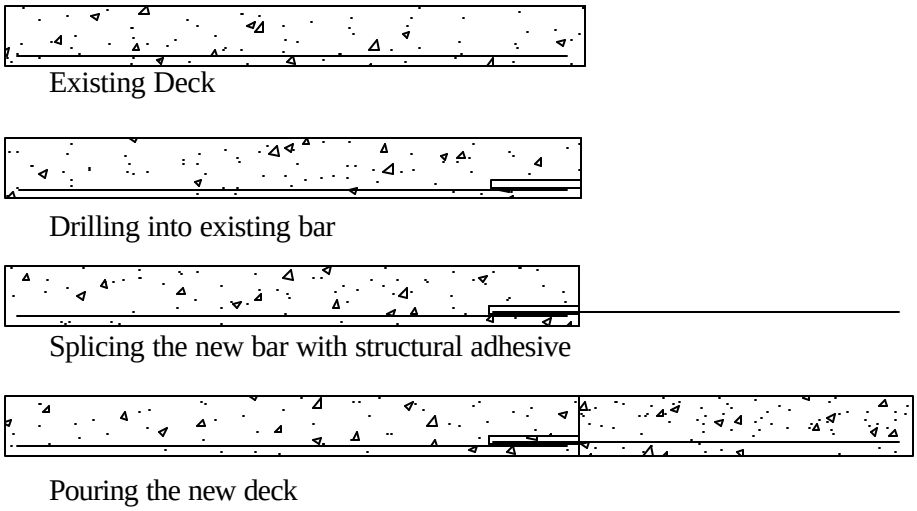

Figure 1.2 – Purposed splicing method for bridge deck addition.

1.2 Purpose and Objectives

The purpose of this study was to investigate the feasibility of using post-installed adhesive-bonded splices for bridge deck additions. The study included both constructability concerns and structural requirements for the splices.

The objectives of this project were to:

Examine the methods used to install adhesive splices and determine if the methods are practical for use on a job site.

Perform flexural tests to determine the splice length required to achieve full flexural strength when using an adhesive-bonded splice.

Perform shear tests to determine the shear strength of adhesive-bonded dowel bars.

Provide design recommendations for splice lengths for adhesive-bonded reinforcement in bridge deck additions.

Provide design recommendations for determining the shear strength of adhesive-bonded dowel bars in bridge decks additions.

1.3 Organization

Chapter Two provides background on development length and splice length equations including four equations for cast-in-place reinforcement and two equations for bonded anchor applications. Chapter Three describes the size, materials, and parameters of the test specimens. Chapter Three also describes the procedures used to cast test specimens, the methods used to install the adhesive splices, and the test setup for the moment and shear tests performed on the specimens. Chapter Four presents the results of the testing program and compares the data to the cast-in-place and bonded anchor equations. Chapter Five summarizes the results, addresses each of the objectives, and presents recommendations.

CHAPTER 2
LITERATURE REVIEW

2.1 General

This chapter provides background on development length and splice length equations. Two equations related to the development and splicing of reinforcing bars and a bonded anchor equation, are presented. The shear friction equation from ACI 318-99[2] is also presented.

2.2 Definitions of Terms

Embedment Length: Length of the embedded reinforcement provided beyond a critical section.

Development Length: Length of the embedded reinforcement required to develop the design tensile strength of the reinforcement at a critical section.

Splice Length: Overlap length of two pieces of reinforcement required to develop the design tensile strength of the reinforcement.

2.3 Background on Splices and Development Lengths

The uniform bond stress model is a basic model that can be used to explain how embedded bars transfer load to the concrete. Figure 2.1 shows a graphical representation of the uniform bond stress model. The application of equilibrium to the model shown in Figure 2.1 yields Equation (2-1). Equation (2-1) can be used to determine the tension force that can be applied to a bar for a given embedment length and bond strength.

Equation (2-2) represents a simple rearrangement of the terms in Equation (2-1) and can be used to determine the embedment length required for a given force.

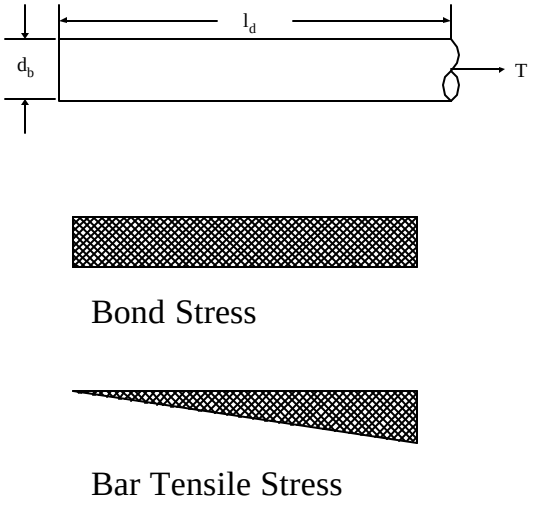

Figure 2.1 – Bond and tensile stresses on a smooth bar with uniform bond stress.

$$T = \delta * d_b * l_d * \hat{o} \tag{2-1}$$

or

$$l_d = \frac{T}{\pi * d_b * \tau} \tag{2-2}$$

l_d = embedment length or development length
T = tensile force
d_b = diameter of the bar
τ = bond stress between bar and concrete

There are two assumptions made for the uniform bond stress model. The first assumption is that the bond stress is uniform (and the tensile stress in the bar is linear) over the entire length of the bar. The second assumption is the bar does not contain deformations[9].

Mains[7] investigated the first assumption, uniform bond stress with linear tensile stress. Initial tests used strain gages that were attached to smooth steel rods to determine the stresses at different locations on the bar. The results showed the bond stress field was uniform and the tensile stress linear on the steel rod for embedment depths 12 inches or less. For longer embedment depths the tensile stress in the bar followed a curved shape as shown in Figure 2.2. These results indicate that the basic assumption of uniform bond stress was incorrect for bars embedded into concrete greater than 12 inches.

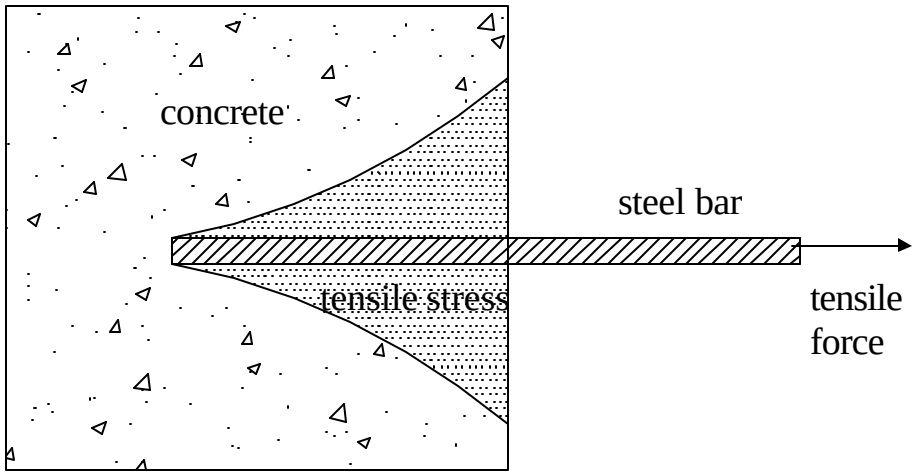

Figure 2.2 – Tensile stress in a bar embedded in concrete

Rehm[9] investigated the second assumption from the uniform bond stress model in studies focused on the use of deformed bars. The deformed bars had ribs that ran along the entire length of the bar as shown in Figure 2.3. By using a deformed bar, additional complexity was introduced.

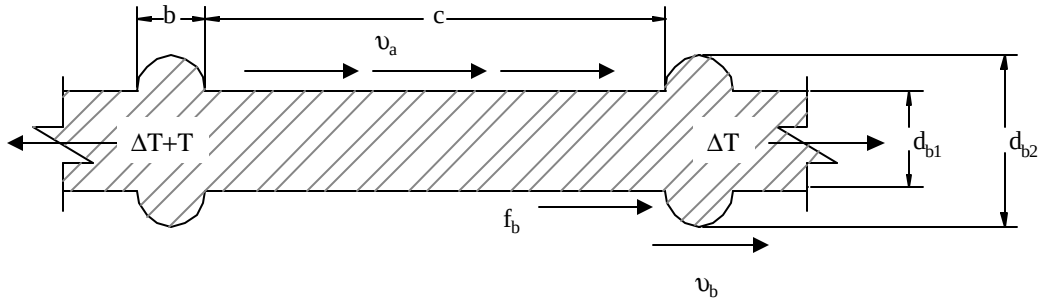

Figure 2.3 - Stresses on a ribbed bar

There are three different types of stresses shown in Figure 2.3: stress due to the adhesion along the surface of the bar υ_a, shear stress from the ribs υ_b, and bearing stress on the ribs f_b. Rehm[9] analyzed one segment of the bar from rib to rib and formulated an equation for the force ΔT developed. The equation has been simplified by assuming the shear stress on the ribs is equal to the shear stress on the surface. Therefore, υ_a is replaced with υ_b and the distance c and b are added together.

$$\Delta T = \pi * d_{b1} * (b + c) * u_b + \pi * \frac{d_{b2} - d_{b1}^{\ 2}}{4} * f_b \qquad (2\text{-}3)$$

DT = incremental force on the bar
d_{b1} = diameter of the bar, excluding ribs
d_{b2} = diameter of the bar including the rib
f_b = bearing stress
u_b = shear stress on ribs
u_a = shear stress between ribs
c = spacing between the ribs
b = width of a rib

By multiplying Equation (2-3) by the total number of segments, the total bar force can be determined.

As new splice equations were formulated, these new equations were still inconsistent in predicting the splice lengths. Due to these inconsistencies, new parameters were

examined to determine what affected the strength of the splices. The testing revealed that the following parameters had an effect on the splice length: strength of concrete, edge effects, and transverse reinforcement. As a result, the equations for development length contained new factors to account for these parameters. Depending on the parameter, a factor was applied to increase or decrease the development length. The influences of each of these parameters are discussed below.

Strength of concrete: In order to increase the embedment strength, the concrete needs to withstand the compressive forces generated at the ribs of the embedded bar. The concrete must also withstand the radial tensile forces caused by tension in the bar. A bar loaded in tension may fail by a breakout failure, a splitting failure, or by the bar yielding. A breakout failure occurs when there are no edge effect problems and when the concrete fails before the bars yields. A splitting failure occurs near edges when radial cracks form in the concrete resulting from the bar trying to pull out. A yielding failure occurs if the embedment is sufficient to preclude the previous two failures. Therefore, the higher strength of the concrete, the greater the transfer of load before an embedment failure is reached.

Edge effects or the clear cover distance: The clear cover is the distance from the closest free edge to the edge of a bar. When a bar is loaded in tension, it transfers the load to the concrete and a radial stress field begins to develop. As the edge distance gets smaller it is more likely that a splitting failure resulting from the radial stress field may develop.

Transverse reinforcement: Transverse reinforcement is typically used for shear strength. However, the confining ability of the reinforcement also increases the tensile strength of the concrete. When a bar has an edge effect condition, as mentioned above, there is an associated reduction of strength of the embedment due to splitting failure. By placing transverse reinforcement in the edge distance problem zones, the resistance to splitting failure is increased and therefore reduces the sudden edge failure.

2.4 Development and Splice Length Equations for Cast-In-Place Reinforcement

The following equations are used to predict the development length of a bar. The first equation (EQ (2-4)) is from ACI 318-99[2]:

$$l_d = \frac{3}{40} * \frac{f_y}{\sqrt{f_c'}} * \frac{\alpha * \beta * \gamma * \lambda}{\frac{c + K_{tr}}{d_b}} * d_b \qquad \frac{c + K_{tr}}{d_b} \le 2.5 \qquad (2\text{-}4)$$

l_d = development length (in)
f_y = rebar yield stress (psi)
f'_c = concrete compressive stress (psi)
α = reinforcement location factor
β = coating factor
γ = reinforcement size factor
λ = lightweight aggregate concrete factor
c = clear cover or edge distance (in)
K_{tr} = transverse reinforcement index,
d_b = diameter of the rebar (in)
A_s = area of the rebar (in^2)

The ACI 318-99[2] applies a 1.3 multiplication factor to achieve a Class B splice. A Class B splice occurs when all of the splices occur in the same location or not staggered. This is the type of splice used in all of the test series.

The second equation (EQ (2-5)) is from AASHTO[1] codes:

$$l_d = \frac{1.25 * A_s * f_y}{\sqrt{f_c'}} \qquad (2\text{-}5)$$

l_d = development length (in)
f_y = rebar yield stress (ksi)
f'_c = concrete compressive stress (ksi)
A_s = area of the rebar (in^2)

The AASHTO[1] code applies a 1.7 multiplication factor to convert the development length to a Class C splice length. Class C occurs when the splice bars are in the same location or not staggered. This is the type of splice used in all of the test series.

Table 2.1 provides a comparison of the two equations based on a concrete strength of 4000-psi, a steel strength of 60-ksi, a diameter of bar of 0.625 inches, a clear edge distance of 2 inches, and no transverse reinforcement.

Table 2.1 – Development length and splice length for the two cast-in-place equations

Cast-In-Place Equations	Development length (inches)	Appropriate splice length factor	Splice length (inches)
ACI (EQ (2-4))	14.2	1.30	18.5
ASSHTO (EQ (2-5)	11.5	1.70	19.5

2.5 Failure Modes of Adhesive-Bonded Bars

As discussed in Cook et al.[3], there are four possible failure modes that may occur when adhesive-bonded bars are placed in tension: bond failure of the adhesive to the bar, bond failure of adhesive to the concrete, concrete splitting, and steel failure. The bond failure of the adhesive to the bar or adhesive to the concrete occurs when the bond strength of the adhesive is not high enough to transfer the load to the concrete. The concrete splitting failure typically occurs when the bar is located near a free edge and

when the radial stresses are large enough to split the concrete. Steel failure occurs only if the first three failure modes do not occur and when the load is large enough to reach the fracture load of the bar.

Based on the results of over 2,900 tests contained in an international database, Cook et al.[4] concluded that the uniform bond stress model provided the best fit to the international database. McVay et al.[8], found that the uniform bond stress model could also be verified by non-linear analytical models. As a result, the uniform bond stress model has been accepted as an appropriate model for single bonded anchors. Based on an extensive testing program involving bonded anchor groups and edge conditions, Lehr and Eligehausen[6] have developed a model that includes factors to account for both group and edge effects as shown below:

$$N_u = \frac{A_n}{A_{n0}} * \Psi_e * N_0 \qquad (2\text{-}6)$$

where:

A_n = projected area at the concrete surface assuming as limited by edges $8\ d_b$ and other anchors if s_{cr} $16\ d_b$ (see Figure 2.4)

$A_{n0} = s_{cr}^{\ 2} = (16 * d_b)^2$ projected area of one anchor not effected by edges

$\Psi_e = 0.7 + 0.3 * \frac{c}{c_{cr}} < 1.0$ edge effect factor

$N_0 = \boldsymbol{p} * d_b * h_{ef} * \boldsymbol{t}$ basic single anchor strength

d_b = diameter of the bar (in)
c = distance to the nearest edge from the centerline of the anchor (in)
c_{cr} = 8 * d_b critical edge distance (in)
h_{ef} = effective embedment depth (in)
s_{cr} = 16 * d_b critical spacing (in)
t = average tensile stress (psi)

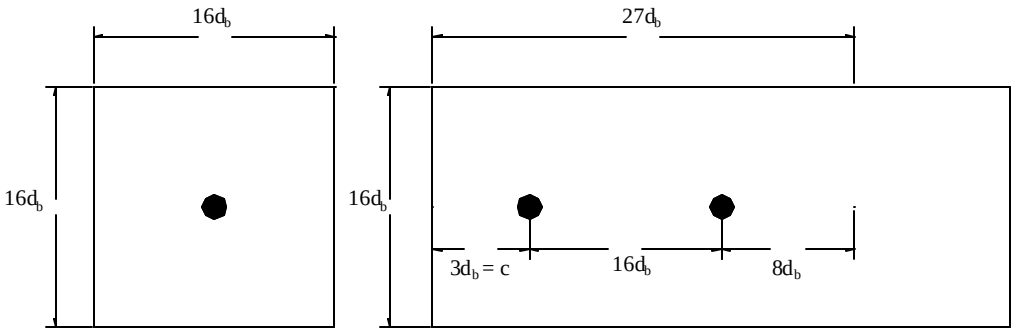

Figure 2.4: Projected area of single anchor (A_{no}) and group of anchors (A_n)

A model similar to that proposed by Lehr and Eligehausen[6], is presented in the FDOT Design Guidelines[5]. This is an earlier model that is based on a limited number of tests. The only differences between the models are in the definition of critical spacing s_{cr} ($2.0h_{ef}$ rather than $16d_b$) and a slight difference in the edge effect factor. Since the Lehr and Eligehausen[6] model represents a more recent model that is based on substantial tests, it is used in the evaluation of the test results for this project. As a note, the FDOT Design Guidelines are to be revised to reflect the changes in the critical spacing and the edge effect factor.

2.6 Shear Strength Equations

In addition to determining the moment capacity of the splice, the shear strength of the splice was also examined. Section 11.7.4.3 of ACI 318-99[2] presents the shear friction Equation (2-7). Shear friction occurs when two surfaces, crossed by reinforcement, try to slip relative to each other. When the concrete attempts to slip, the roughness of the slip

plane causes the splice bars to be put into tension providing a normal force across the shear plane resulting in a frictional resistance. ACI 318 shear friction equation is:

$$V_n = A_{vt} * f_y * m \quad (2\text{-}7)$$

A_{vt} = area of the bar normal to the concrete surface
f_y = yield stress of the bar
m = 1.4 for a monolithic pour
= 1.0 for concrete placed against hardened concrete with surface intentionally roughened
= 0.6 when placed against hardened concrete not intentionally roughened
= 0.7 when concrete is anchored to as-rolled structural steel by headed studs or by reinforcing bars

For this project there was no treatment to the formed slab face before the second half was poured, therefore m was taken as 0.6.

2.7 Summary of Literature Review

This chapter has presented information on development length and splice length equations. Two cast-in-place equations and a bonded anchor equation were presented.

CHAPTER 3
CONSTRUCTION, INSTALLATION, AND TEST PROCEDURE

3.1 General

Chapter 3 discusses the construction of the formwork, casting of the concrete, installation of the splice bars, and testing procedure used for this project.

3.2 Specimen Size

The dimensions of the specimens are shown in Figure 3.1 . The length of the specimen was determined by the required splice length in the AASHTO code, plus the minimum required development length of the reinforcement on each side of the splice.

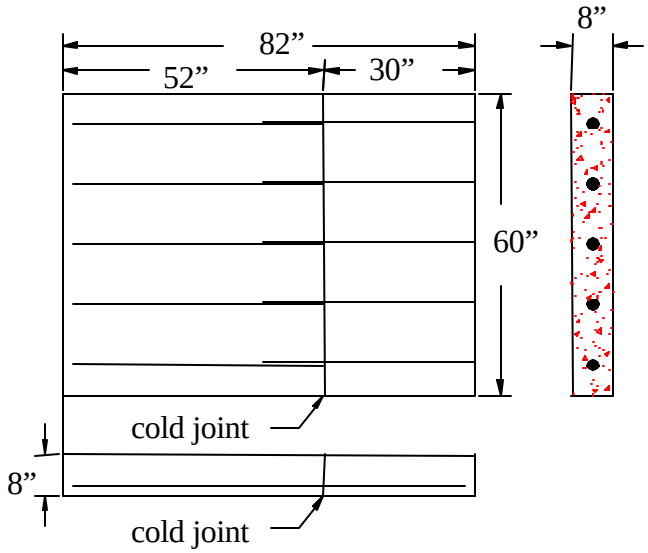

Figure 3.1 – Dimensions of the test specimens

The 60-inch width was determined from five #5 bars spaced at 12 inches on center. The 8-inch thickness is a standard bridge deck thickness.

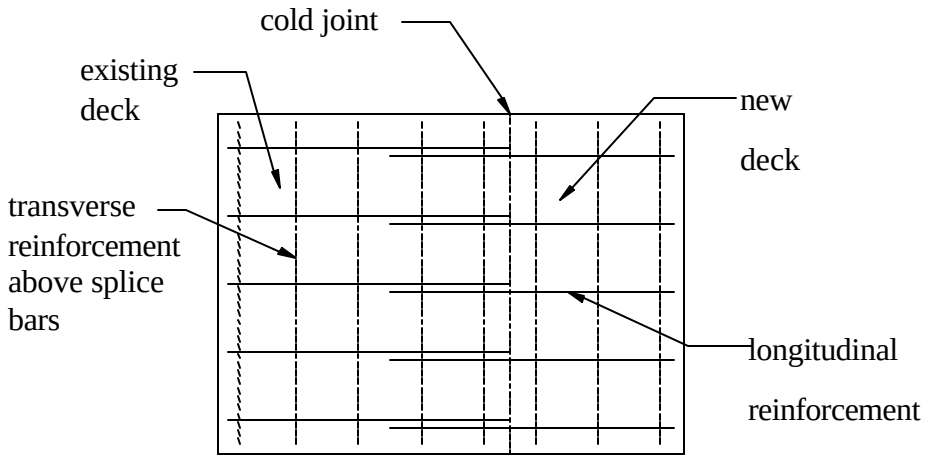

Figure 3.2 – Typical reinforcement layout for the specimens

3.3 Specimen Parameters and Variations

There were four series of tests conducted with five specimens in each series. In each series five blocks were cast, a control specimen, and four specimens with varying parameters. Table 3.1 shows the specimen's designations and the type of test performed for Test Series 1-3. Table 3.2 shows the specimen's designation and type of test performed for Test Series 4.

Table 3.1 – Test Series 1-3

Test Series 1-3	Test Performed	Bar Splice Location	Figure
Control	Moment	none	
Specimen A	Moment	next to existing bars	3.3
Specimen B	Moment	between existing bars	3.4
Specimen C	Moment	above existing bars at center of slab	3.5
Specimen D	Shear	above existing bars at center of slab	3.5

1. Test Series 1, Specimen B only had a 4 bar splice. The splice bar located 3" from the edge of the specimen was included in this specimen.

Table 3.2 – Test Series 4

Test Series 4	Test Performed	Bar Splice	Figure
Control	Moment	none	
Specimen A	Moment	16” embed at 12” spacing, in between existing bars	3.4
Specimen B	Moment	16” embed at 8” spacing, next to existing bars	3.6
Specimen C	Moment	12” embed at 12” spacing, in between existing bars	3.4
Specimen D	Moment	12” embed at 8” spacing, next to existing bars	3.6

Parameters were varied for each test series and each specimen. One parameter varied was the embedment length. The first embedment length for test Series 1 was determined assuming 4000 psi concrete and #5 Grade 60 rebar. Using the AASHTO equation the splice length was 19.4 inches. As a result, the embedment length for Test Series 1 was 20 inches. The next two Test Series embedment lengths were 15 and 11 inches. Test Series 4 had embedment lengths of 12 and 16 inches as shown in Table 3.2. Table 3.3 provides a summary of the embedment lengths used for the four test series.

Table 3.3 – Test series embedment length

Test Series	Embedment Length
Series 1	20 inches
Series 2	15 inches
Series 3	11 inches
Series 4	16 and 12 inches

Another parameter varied was the location of the splice as indicated in Table 3.1 for Test Series 1-3. For Test Series 4 the new bars were installed next to the existing bars. The final parameter varied was the clear spacing; this change was only conducted in Test Series 4. Specimens A and C used a 12” spacing of reinforcement as shown in Figure 3.3

while Specimens B and D used an 8” spacing as shown in Figure 3.6. This increased the distance to a free edge.

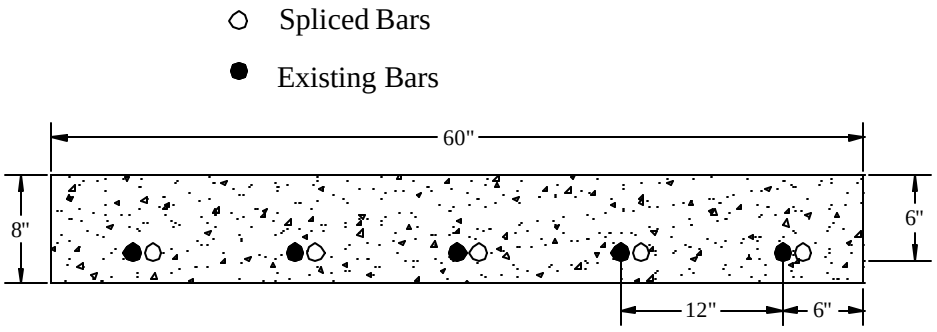

Figure 3.3 – Test Series 1-3, Specimen A reinforcement spacing and depth

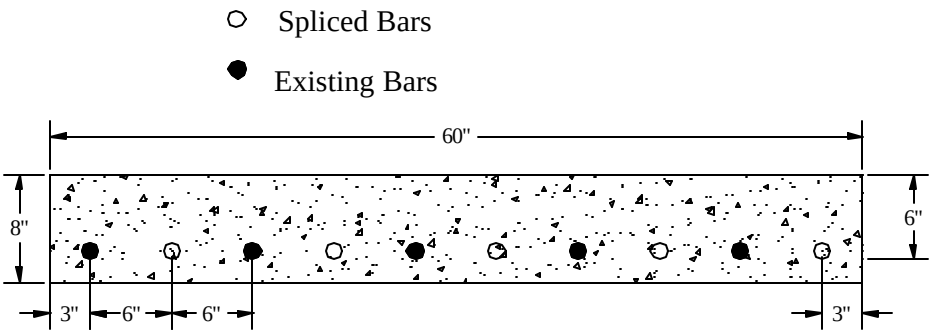

Figure 3.4 – Test Series 1 - 3, Specimen B reinforcement spacing and depth.

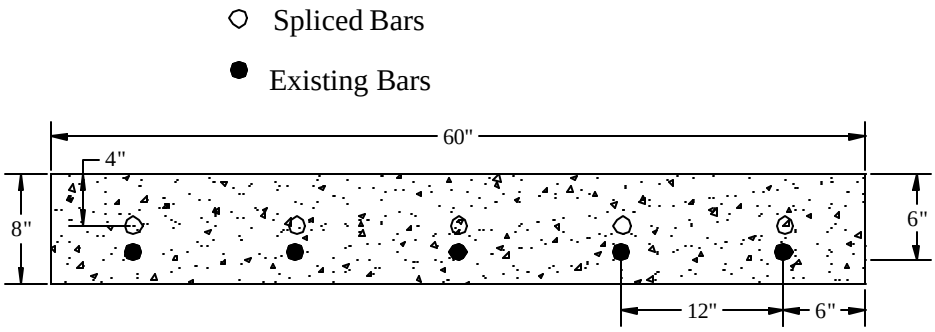

Figure 3.5 – Test Series 1-3, Specimen C and D reinforcement spacing and depth

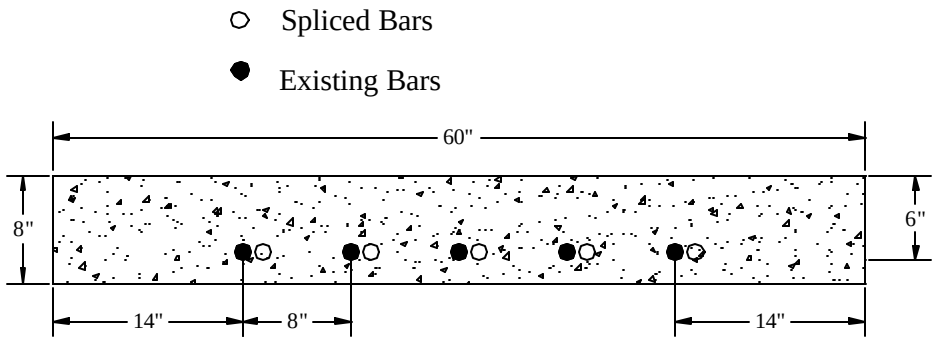

Figure 3.6 – Test Series 4, Specimen B and D reinforcement spacing and depth

For Test Series 1, Specimen B had four bars spliced in between each rebar in order to avoid and edge distance factors. However, since one of the objectives for this research was to determine the possible effects of any edge distance factor, the remaining test series used five bar splices as shown above in Figure 3.3 through Figure 3.6.

3.4 Reinforcement

The tensile strength of the reinforcement was varied between Test Series 4 and Test Series 1-3. Table 3.4 shows the average tested yield stress for the reinforcement for each of the test series. Each Test Series had 3 #5 bars tested.

Table 3.4 – Actual yield stress of the reinforcement used for each test series

Test series	Yield Stress (ksi)
1	45.5
2	52.6
3	52.1
4	67.6

3.5 Adhesive-Bond Stress Tests

A baseline test was conducted to determine the average bond stress of the adhesive. The type of adhesive was a two part adhesive with a self-mixing nozzle. Five 67-ksi rebars were embedded 3.5 inches into an 8" thick concrete specimen with a 28-day concrete compressive strength of 4142-psi. All five bars had an unconfined pull-out test conducted to determine the failure load of the epoxy. The test consisted of applying an tension force on the anchor until the anchor failed. A bond failure occurred for all five specimens. The pull-out loads and the average bond stress are shown in

Table 3.5 . Equation (3.1) was used to calculate the average bond stress (τ) for the epoxy.

$$\tau = \frac{P_u}{h_{ef} * d_b * \pi} \tag{3.1}$$

P_u = average pull-out load

h_{ef} = effective embedment depth

d_b = diameter of the bar

Table 3.5 – Pull-out loads and average bond stress for the epoxy

Baseline tests	Pull-out load (lbs)	Bond stress (psi)
Pull-out test 1	11568	1682
Pull-out test 2	12375	1799
Pull-out test 3	13655	1986
Pull-out test 4	13023	1894
Pull-out test 5	13679	1989
	Average =	1870
	Standard deviation =	131
	Coefficient of variation =	0.07

3.6 Concrete Types and Strengths

The concrete for Test Series 1-3 was an FDOT Class II concrete with a minimum specified compressive strength of 3,400-psi. The mix included cement, slag, sand, 57 stone, MBRV, MBl80, and water. However, the actual 28-day compressive strength was much greater as shown in Table 3.6 . For Test Series 4 a different concrete mix was used so that the 28-day compressive strength would be about 4,000-psi. Table 3.6 shows the actual concrete compressive strength for each series at 28-days and at the time of testing. The concrete compressive strength curves can be found in the Appendices A-D for each series. Tests of the compressive strength of the concrete cylinders were conducted at 7, 14, 21, and 28 days. Additional compressive strength tests were conducted when each specimen was tested, Table 3.6 and Table 3.7 .

Table 3.6 – Concrete compressive strength

Pour 1, Test Series (Representing the old deck)	28-day strength (psi)	Strength at time of tests (psi)
1	7501	8310
2	7276	8318
3	6828	8160
4	4063	4142

Table 3.7 – Concrete compressive strength

Pour 2, Test Series (Representing the new deck)	28-day strength (psi)	Strength at time of tests (psi)
1	7121	7458
2	6926	7649
3	7160	8127
4	4102	4102

3.7 General Discussion of Materials

Two unanticipated concerns developed in the course of the testing program. For Test Series 1-3 the actual concrete strength of the FDOT Class II concrete (that has a specified minimum compressive strength of 3,400-psi) was over 7,000-psi at 28 days and 8,000-psi at the time of testing (see Table 3.6 and Table 3.7). Although the most commonly supplied FDOT Class II concrete was ordered from the supplier, the current mix designs provided for FDOT jobs contain significantly more cementitious and/or pozzolan materials to ensure corrosion protection than that necessary to provide the minimum specified strength of 3,400 psi. This problem was corrected in Test Series 4 by ordering concrete mix with an anticipated 28 day strength of 4,000 psi (actual 28 day strength and at the time of testing was 4,102 psi).

For Test Series 1-3, the design of the test specimens was based on #5 GR 60 reinforcement. Inadvertently, the supplier furnished #5 GR 40 reinforcement with an actual yield strength of ~50 ksi (see Table 3.5). This was corrected in Test Series 4 that utilized GR 60 reinforcement with an actual yield strength of 67.6 ksi.

3.8 Concrete Casting Procedure

The specimens were cast by placing concrete in the forms and vibrating the concrete until few air bubbles were visible. The concrete was then screeded and troweled to a smooth finish. Once the concrete set up, burlap was placed over the specimens and kept damp for seven days. Thirty concrete cylinders were also cast and cured in the same area as the test specimens. After seven days, the burlap, forms, and cylinder molds were removed. The cylinders and concrete specimens were left to cure for 28 days. Following

the 28 days, the splice dowels were installed and the second portion of the deck was poured and cured for 28 days using the same procedure.

3.9 Post-Installed Splice Procedure

The splice bars were standard #5 bars installed using a 3/4-inch diameter drill bit that allowed a 1/8-inch over-sized hole as recommended by the epoxy manufacturer. The holes were marked on the face of the block and a drilling guide was constructed to help position and guide the bit. The drilling guide was made of wood and shaped like the block letter "P" as shown in Figure 3.7 . The leg of the letter "P" was placed on top of the specimen and the square end was butted up to the face of the specimen. The holes in the drilling guide were at a 4-inch and 6-inch depth. The drilling guide was stabilized on the concrete using 50-pound weights, two on the leg of the drilling apparatus and one on each side to prevent movement while drilling. Once the apparatus was in place, a hammer drill was used to drill the holes.

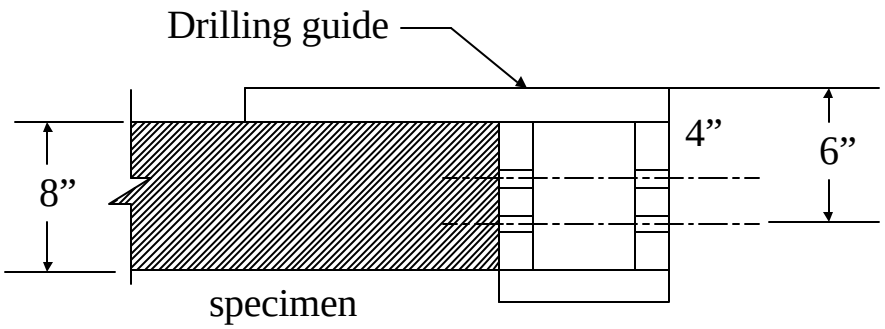

Figure 3.7 –Drilling guide

After drilling was finished, the holes were cleaned with a bristle brush and then blown clean with 60-psi compressed air. This procedure of brushing and blowing was repeated three times for each hole. Once the hole was cleaned, it was taped closed. Once all the

holes on a specimen were cleaned, the tape was removed and the installation of the rebars occurred.

The epoxy was inserted from the back of the hole to the front. The splice bar was installed by slowly twisting the bar farther in until the embedment length was reached, see Figure 3.8 .

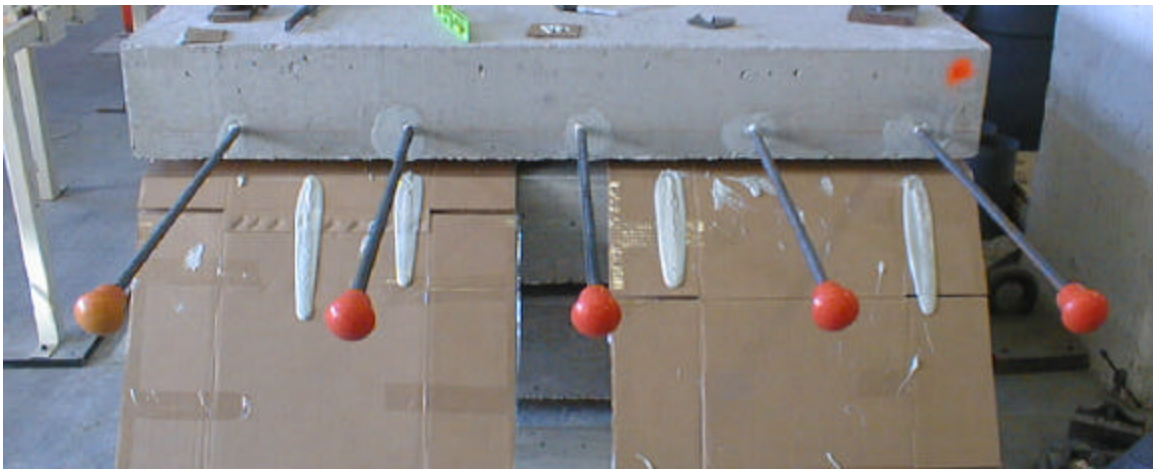

Figure 3.8 – Installed splice bars

The bar was checked to see if it was level, if not, the bar was held in place for a few minutes until the epoxy set. A sample of the epoxies used was taken at the beginning and end of this procedure, to ensure the epoxy was properly mixed. All of the samples were visually checked to verify a proper mix. A gray color indicated a proper mix of the epoxy, which was present in all of the samples.

The time required for the installations for Test Series 1-3 were measured. The three embedment lengths used were: 20-inch, 15-inch, and 11-inch. The 20-inch installation was the most difficult because of its length. The time of drilling was approximately 17-19 minutes per hole. A second person was required for the 20-inch installation to assist in drilling the hole straight and keeping the drill level due to the length of the drill bit. In addition, the drill bit had to be removed twice in order to remove the concrete dust

accumulating on the drill. Both the 11-inch and 15-inch hole depths were easier to drill than the 20-inch hole depth. The drilling time was approximately 7-9 minutes per hole. At this depth, the drill never had to be removed from the hole. In addition, a second person was not required to help the person drilling. The cleaning time for each hole was approximately 2 minutes.

3.10 Testing Procedure

There were two types of tests conducted, a moment test and a shear test. Both tests used a data acquisition device, LVDT's, 100-kip load cell, 120-kip ram, manual hydraulic pump, and a testing frame.

The testing frame consisted of two W12x50 columns and a doubly symmetric channel, as the header connecting to both columns. The columns were bolted to the floor giving a capacity of 100-kips. The ram was attached to the header with the piston pointed to the ground. This basic set up was the same for both types of tests.

3.11 Flexure Test Setup

The moment test was a two-point test as shown in Figure 3.9 . This two-point test was used to achieve a constant moment in the splice region as shown in Figure 3.10 . As shown in Figure 3.11 the setup consisted of using two concrete blocks as a foundation. Rollers were constructed of ½inch flat stock welded to a 1-inch steel rod. These rollers were placed on the foundation blocks 78 inches apart, with the flat plate on the bottom. The specimen was then placed on the rollers with the specimen overhanging 2 inches on each side. Next, two more rollers were placed on the deck at 22 ½inches from the each end of the specimen. These rollers were placed with the 1-inch bar on the bottom in

order to achieve a line load on the specimen. A strip of neoprene was placed under each roller to help smooth out any imperfection on the specimen surface and to reduce any horizontal friction forces that might develop. Once the rollers were in place, the steel loading frame was placed on the rollers. The loading frame consisted of four W14x31 members and a double channel to distribute the load from the ram to the rollers. A load cell was then centered on the channel and a pivoting plate was used to ensure the load was transferred correctly, Figure 3.12 .

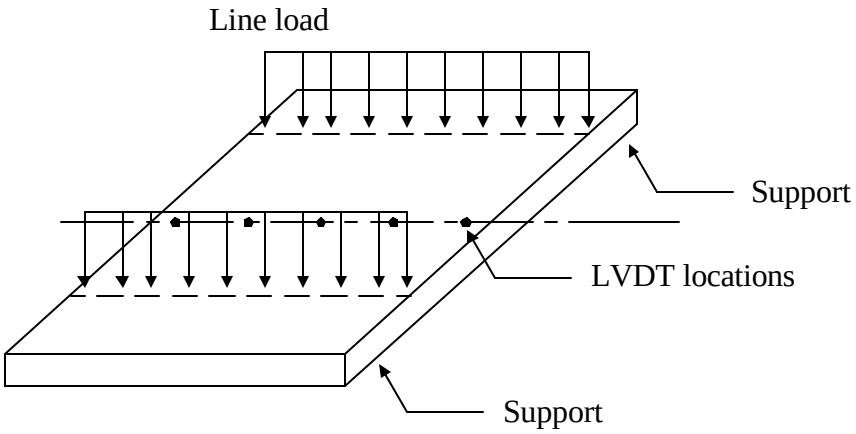

Figure 3.9 – Two-Point loading for moment test

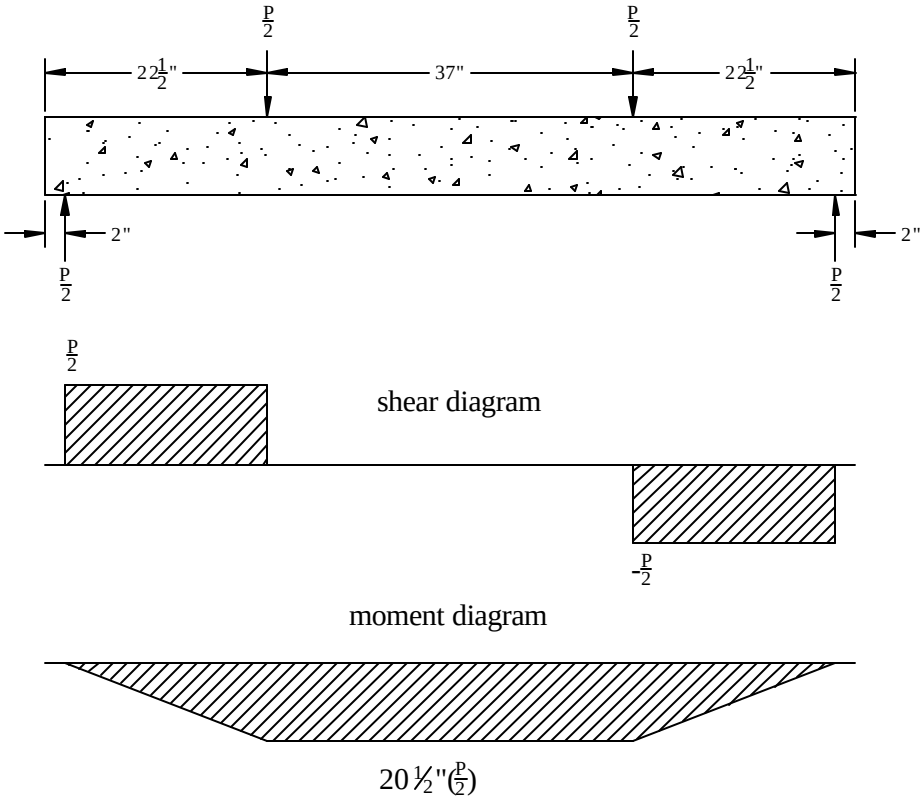

Figure 3.10 – Moment diagram for the moment test

Figure 3.11 – Loading apparatus

Once assembled, the ram was lowered to apply a small amount of pressure to hold everything in place. Next, a small angle frame was used to hold five LVDT's across the specimen. The frame rested on the concrete support and extended across the length of the specimen. In the middle of the specimen's span an angle was attached that crossed the specimen. The angle had five holes drilled at 12" on center that held the LVDT's in place.

Figure 3.12 Ram and load cell on doubly symmetric channel

3.12 Shear Test Setup

The shear test setup was similar to the moment test setup with the difference in the placement of the rollers. Figure 3.13 and

Figure 3.14 show the shear test set up. The first roller was placed 22 inches from the left edge of the specimen. The second roller was placed 52 inches from the first roller or 8 inches from the right side of the specimen. The two reactions points were at 8 inches and at 46 inches from the left side. The line load closest to the cold joint was 4 times greater then the far line load. This was needed to achieve the pure shear zone (approximately no moment) at the splice, Figure 3.13 . For the shear test, two angles

spanned the specimen with three LVDT's supported by each angle, Figure 3.15. Each angle was located 2 inches on each side of the cold joint.

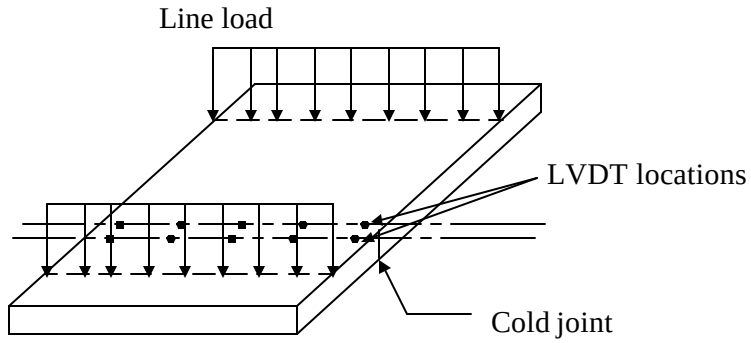

Figure 3.13 – Loading for shear test

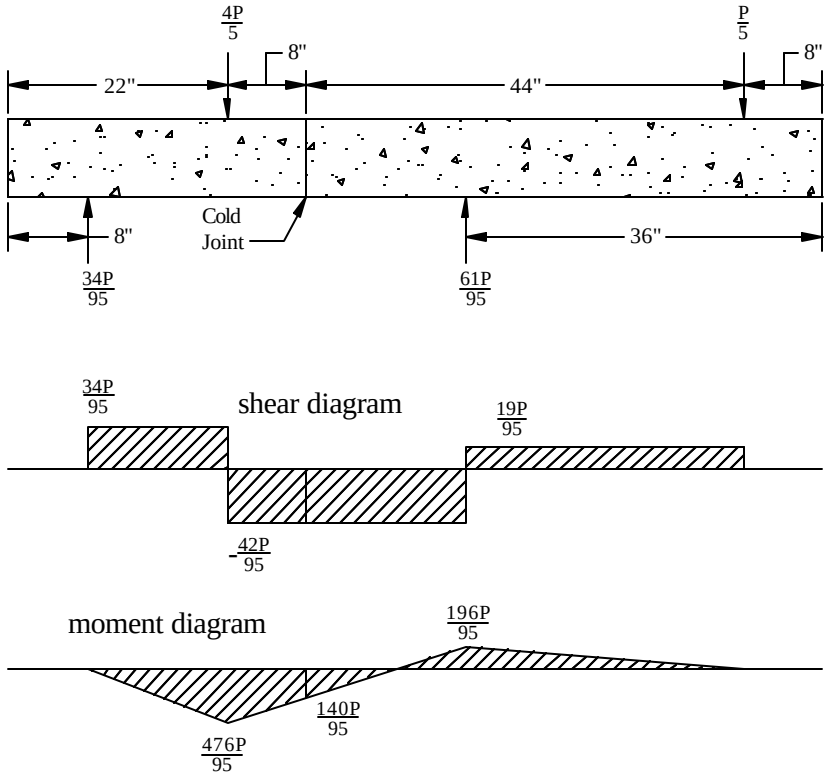

Figure 3.14 –Shear diagram for shear test

Figure 3.15 – Two angles with LVDT's were used on the shear test

CHAPTER 4
TEST RESULTS

4.1 General

This chapter presents the results of the four test series described in Chapter 3. Graphs and photos of Test Series 1, 2, 3, and 4 can be found in Appendix A, B, C and, D, respectively, along with the concrete strength graphs. The forces shown in all of the tables and graphs are the loads recorded by the load cell below the hydraulic ram. All loads designated as $P_{experiment}$ are based on the loads recorded when yielding of the specimen occurred. When the yielding of the specimen was not easily seen the yielding load was determined from the load versus displacement graphs. $P_{experiment}$ is the yielding load for the specimen. For Test Series 1-3 Specimens A-C and Test Series 4 Specimens A-D the $P_{calculated}$ is the theoretical load based on the Whitney stress block. For Test Series 1-3 Specimen D the $P_{calculated}$ is the theoretical load based on the Shear Friction provisions of ACI 318. For all of the tests, *f'c* represents the compressive strength of the specimen in which the embedded bars were epoxied.

4.2 Test Series 1 Results

The first test series had an embedment length of 20 inches. The results for Test Series 1 and failure modes are shown in Table 4.1 and Figure 4.1 .

Table 4.1 – Results for Test Series 1 using actual f_y and f'_c

Series 1 results	$P_{experiment}$ (kips)	$P_{calculated}$ (kips)	$P_{experiment}/P_{calculated}$	Failure mode
Control Specimen	41.5	40.1	1.03	Not fully loaded due to apparatus failure
Specimen A	42.5	40.1	1.05	Flexural crushing of concrete
Specimen B	38.0	32.2	1.17	Flexural crushing of concrete
Specimen C	18.5	19.5	0.95	Flexural crushing of concrete
Specimen D	38.2	33.4	1.15	Concrete shear splitting at control joint

For Specimen B only four bars were spliced and therefore, the $P_{calculated}$ is a lower value than Specimen A. As shown in Table 4.1 the Control Specimen, Specimen A, Specimen B, and Specimen C all reached the calculated flexure load.

Specimen D, the shear test specimen, sheared the control joint at a load slightly greater than the calculated shear friction load. The shear test showed no signs of bond failure or edge effects problems.

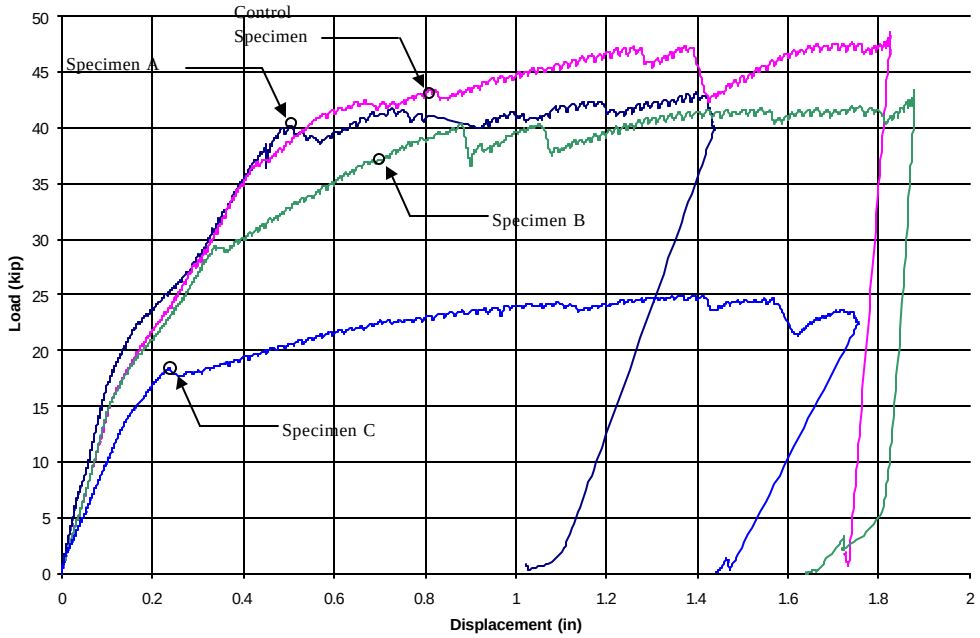

Figure 4.1 – Results from Test Series 1 moment tests

4.3 Test Series 2 Results

The second test series had an embedment length of 15 inches. The results for Test Series 2 and the failure modes are shown in Table 4.2 and Figure 4.2 .

Table 4.2 – Results of Test Series 2 using actual f_y and f'_c

Series 2 results	$P_{experiment}$ (kips)	$P_{calculated}$ (kips)	$P_{experiment}/P_{calculated}$	Failure mode
Control Specimen	33.3	42.2	0.79	Instrumentation error
Specimen A	42.0	42.2	0.99	Flexural crushing of concrete
Specimen B	42.6	42.2	1.01	Flexural crushing of concrete
Specimen C	24.4	22.4	1.08	Flexural crushing of concrete
Specimen D	39.9	35.0	1.14	Concrete shear splitting at control joint

The Control Specimen for this test did not reach the calculated load. The Control Specimen visually did yield and showed all of the same characteristics as Test Series 1 Control Specimen except for the load. Upon further inspection, the location of the reinforcing was correct and the instrumentation was working correctly. No definite answer could be found to explain the results. Specimen A, Specimen B, and Specimen C reached the calculated load and exhibited ductility consistent with the control specimen.

Specimen D, the shear test specimen, sheared at the control joint at a load slightly greater than the calculated shear friction load. The shear test showed no signs of bond failure or edge effects problems.

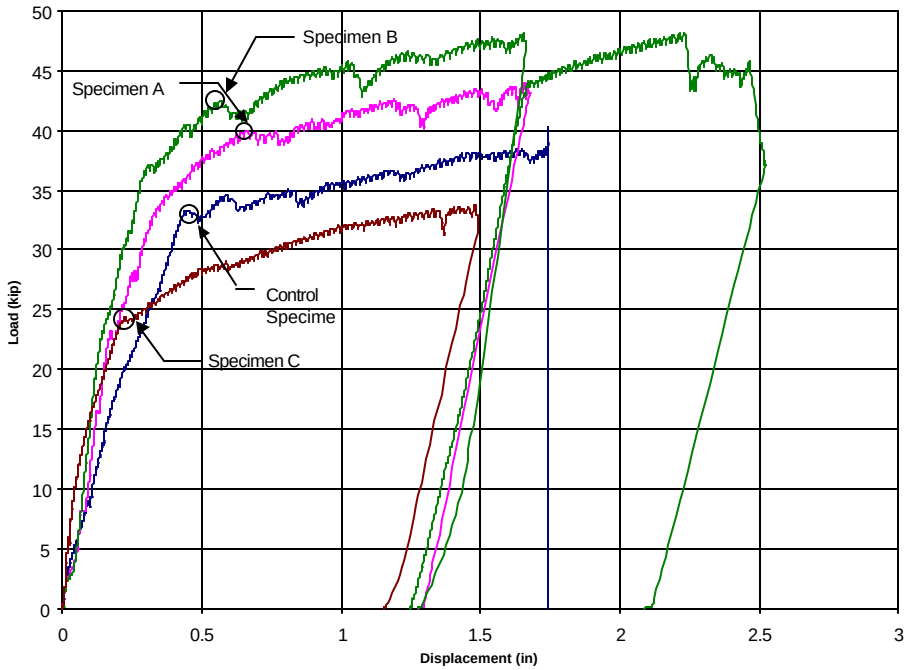

Figure 4.2 – Results for Test Series 2 moment tests

4.4 Test Series 3 Results

The third test series had an embedment length of 11 inches. The results for Test Series 3 and failure modes are shown in Table 4.3 and Figure 4.4 .

Table 4.3 – Results of Test Series 3 using actual f_y and f'_c

Test results	$P_{experiment}$ (kips)	$P_{calculated}$ (kips)	$P_{experiment}/P_{calculated}$	Failure Mode
Control Specimen	42.0	42.1	1.02	Flexural crushing of concrete
Specimen A	40.8	42.1	0.97	Concrete splitting at edge joint
Specimen B	41.4	42.1	0.98	Concrete splitting at edge joint
Specimen C	24.0	22.4	1.07	Flexural crushing of concrete
Specimen D	40.7	35.0	1.17	Concrete shear splitting at control joint

The Control Specimen, Specimen A, Specimen B, and Specimen C all reached the calculated load. As indicated by Table 4.3 , Specimens A and B had edge effect failures after the calculated load but before a concrete compression failure occurred. As shown in Figure 4.4, this resulted in a reduced ductility from that exhibited by the control specimen.

Figure 4.3 – Edge failure of Specimen B

Cracks formed at the top and bottom of the specimen and sloped toward each other forming the shape of a triangle, Figure 4.3. This splitting failure was cause by the high stresses developed in the splice region near a free edge. Therefore, a new arrangement of

the reinforcement was developed to eliminate the edge distance parameter. This was investigated in Test Series 4.

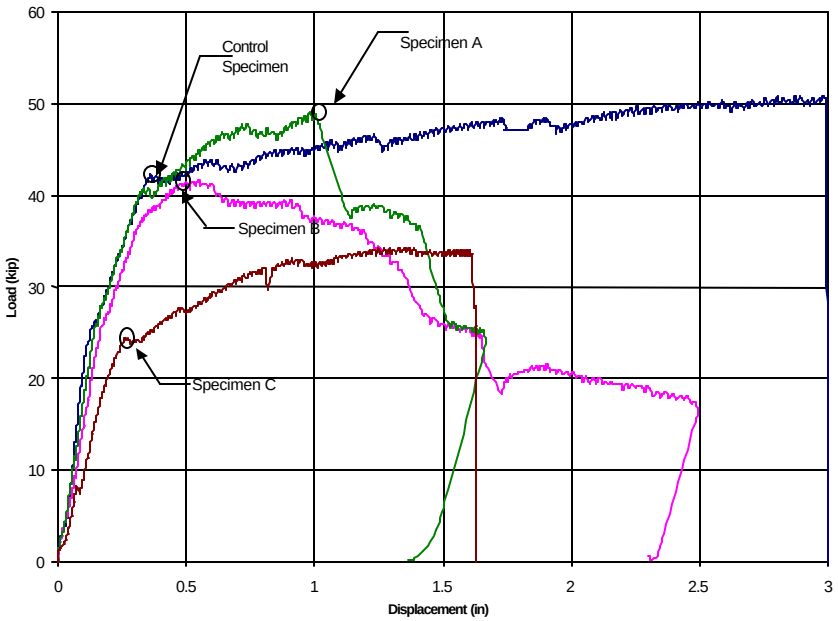

Figure 4.4 – Results for Test Series 3

Specimen D, the shear test specimen, sheared the control joint at a load slightly greater than the calculated shear friction load. The shear test showed no signs of bond failure or edge effects problems.

4.5 Test Series 4 Results

Test Series 4 was conducted for three reasons. The first reason was to test the splice bar with the distance to a free edge greater than 8 bar diameters and see if an edge failure occurred. Second, to determine if the use of Grade 60 bar would affect the accuracy of the equations used to predict the splice lengths. Third, to see if changing the actual concrete compressive strength to 4,000 psi, instead of the ~8000 psi, would affect the accuracy of the equations.

Test Series 4 consisted of one control specimen and four moment tests. No shear test was performed because the data from the previous tests were consistent. The results for Test Series 4 and failure modes are shown in Table 4.4 and Figure 4.5 :

Table 4.4 – Results of Test Series 4 using actual f_y and f'_c

Test results	$P_{experiment}$ (kips)	$P_{calculated}$ (kips)	$P_{experiment}/P_{calculated}$	Failure Mode
Control Specimen	53.9	52.4	1.03	Flexural crushing of concrete
Specimen A	52.6	52.4	1.00	Bond failure
Specimen B	50.9	52.4	0.97	Bond failure
Specimen C	48.8	52.4	0.93	Bond failure
Specimen D	38.7	52.4	0.74	Bond failure

The Control Specimen for Test Series 4 reached the calculated yield load. Specimen A, Specimen B, Specimen C, Specimen D all had sudden bond failure before yielding as shown in Figure 4.5 indicating a brittle failure mode. These specimens all had radial cracks on the bottom surface of the specimen, Figure D.1 – D.4.

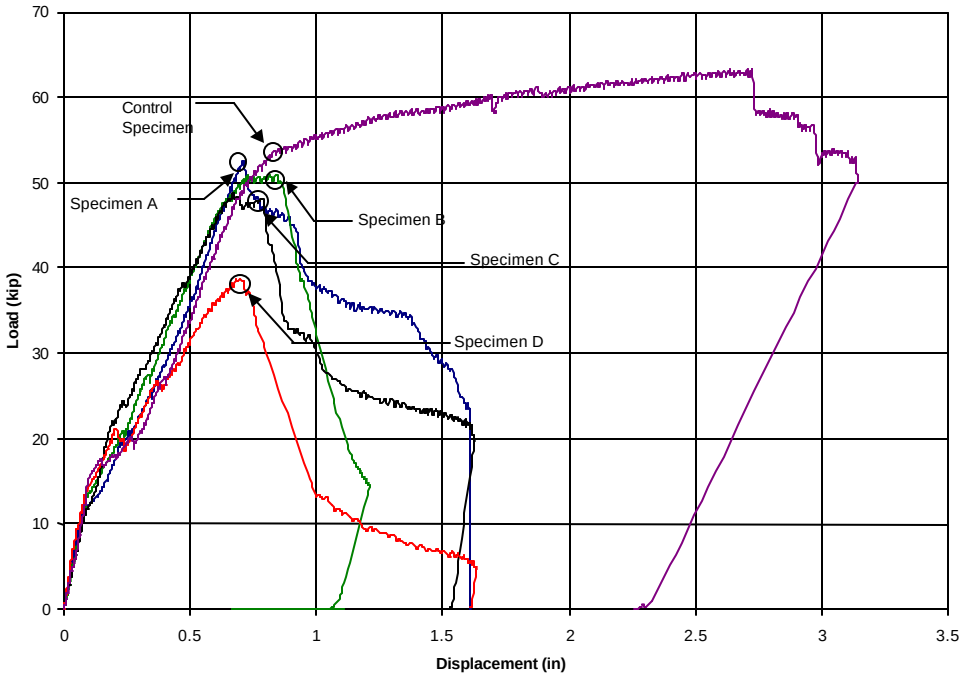

Figure 4.5 – Results from Test Series 4

4.6 Comparison of Test Results

Graphs of the results comparing all of the specimens in a particular test series and a comparison of like specimens from each test series can be found in Appendix E. Figure E.1-E.3 show the specimen's stiffness with post-installed epoxy splices were consistent with the stiffness of the control specimen.

Two types of rebar splices were used in this project, bars spliced next to the existing bars (Specimen A) or spliced in-between the existing bars (Specimen B). These two variations were conducted to see if the specimen's strength would be affected. Table 4.5 compares the yielding loads of the specimens with different rebar splice locations. Test Series 1 is not used for comparison because only 4 bars were spliced in Specimen B and five bars were spliced in Specimen A.

Table 4.5 – Comparison of specimens with different spacing of splices.

Specimen	Spacing	Test Series 2 l_d = 15in	Test Series 3 l_d = 11in
A	Next to existing bar	42.0	40.8
B	In between existing bar	42.6	41.4
	Percent difference	1.43%	1.47%

As shown in Table 4.5 the spacing of the bars had little affect on the strength of the specimen.

4.7 Splice Equation Comparison

Table 4.6 shows the splice lengths calculations for ACI[2], AASHTO[1], and Eligehausen's[6] equations using the actual strength of the materials at the time of testing. As previously discussed in Section 3.7, due to the use of Grade 40 bars and a concrete strength of ~8000-psi the embedment lengths were greater than the predicted splice lengths for Test Series 1 and 2. Therefore, no good comparisons could be made to the splice length equations for Test Series 1 and 2. As noted in the notes on Table 4.6, the ACI and AASHTO equations for splice length contain both a built in capacity reduction factor (ϕ) on the development length of ~0.9 and multipliers of 1.3 for ACI and 1.7 for AASHTO to convert the development length to a splice length. These factors are not included in the Eligehausen's equation but recommended values are addressed at the end of this section.

Table 4.6 – Required splice lengths based on actual material strengths

Test Series	f_y (ksi)	f'_c (ksi)	Splice (in)	τ (ksi)	ACI[1] (in)	AASHTO[2] (in)	Eligehausen[3] (in)	Yielding or Bond Failure
1	45.5	8.31	20	1.87	9.7	10.4	7.0	Yielding
2	52.6	8.32	15	1.87	11.2	12.0	8.1	Yielding
3	52.1	8.16	11	1.87	11.2	12.0	8.0	Yielding
4-A	67.6	4.14	16	1.87	20.5	21.9	11.3	Bond Failure
4-B	67.6	4.14	16	1.87	20.5	21.9	10.4	Bond Failure
4-C	67.6	4.14	12	1.87	20.5	21.9	11.3	Bond Failure
4-D	67.6	4.14	12	1.87	20.5	21.9	10.4	Bond Failure

1. Contains a built in capacity reduction factor (ϕ) of ~0.9 and a splice length factor of 1.3 for converting development length to splice length.
2. Contains a built in capacity reduction factor (ϕ) of ~0.9 and a splice length factor of 1.7 for converting development length to splice length.
3. Does not contain a built in capacity reduction factor or a factor for converting development length to splice length.

As shown in Table 4.6 , Test Series 3 had an embedment length of 11 inches. Both ACI and AASHTO equations required a splice length of 11.2 and 12 inches, respectively. Therefore, both the ACI and AASHTO equations predicted safe and conservative splice lengths for the testing parameters of Test Series 3 since yielding occurred prior to failure. It should be noted that the ductility of Specimen B was reduced from that of the Control Specimen and Specimen A. The embedment length for Test Series 3 was larger than the predicted length of Eligehausen's equation without the introduction of the capacity reduction factor (ϕ) and multiplier for determining splice length as included in the ACI and AASHTO equations.

Test Series 4 had embedment lengths of 12 and 16 inches. ACI and AASHTO equations predicted splice lengths of 20.5 and 21.9 inches, much greater than the embedment length for Test Series 4. Table 4.4 shows that Test Series 4 Specimens A through Specimens D had a bond failure before yielding occurred. However, Table 4.4 also shows that Specimens A, B, and C were very close to their calculated yield load but

without the ductility exhibited by the Control Specimen. It is suggested that an additional Test Series be performed to verify the modifications factors and splice lengths predicted by ACI and AASHTO equations.

Eligehausen's equations predicted a splice length of 10.4 inches and 11.3 inches for the 12 and 16-inch embedment lengths of Test Series 4, respectively. Therefore, for Test Series 4 results, Eligehausen's equation is not adequate without the incorporation of a capacity reduction factor (ϕ) and multiplier for converting development length to splice length as used in ACI and AASHTO.

As mentioned above, when comparing ACI and AASHTO equations to Eligehausen's equation, two issues needed to be addressed. Both the ACI and AASHTO equations have a capacity factor (ϕ) 0.9 built into the equations. Also, both ACI and AASHTO splice length equations are development length equations with multiplication factors of 1.3 or 1.7, respectively. Eligehausen's equation does not have a built in capacity reduction factor and is a development length equation. Therefore, to accurately compare Eligehausen's equation to ACI and AASHTO equations, a capacity reduction factor of 0.9 should be applied to Eligehausen's equation (this amounts to multiplying the predicted development length by $1/0.9 = 1.11$). After the capacity reduction factor is applied, a second factor needs to be applied, or in this case determined, in order to convert Eligehausen's development length equation to a splice length equation. This factor should enable Eligehausen's equation to safely predict the splice length tested in Test Series 4. Specimens A of Test Series 4 had an embedment length of 16 inches and a rebar spacing of 12 inches. Since Specimen A was at the predicted yielding failure load, the embedment length of 16 inches will be used determine the factor to convert

Eligehausen's development length equation to a splice length equation. Eligehausen's equation predicted an embedment length of 10.4 inches. Therefore, divide 10.4 inches by the 0.9 factor. This new length is 11.6 inches. Next divide the embedment length of 16 inches by 11.6. The result is a 1.38 factor. By rounding up 1.38 to 1.4, the factor can be used to convert Eligehausen's development length equation to a splice length equation. The 1.4 multiplier for splice length factor is derived from a test specimen that had a sudden catastrophic failure. For safety concerns a factor based on a yielding failure is preferred. However, since all of the specimens of Test Series 4 had a sudden catastrophic failure, additional test may need to be performed to verify the reliability of the derived 1.4 multiplier for splice length factor. Therefore, based on Test Series 4, is appears reasonable that both of these factors, a capacity reduction factor of 0.9 and a multiplier for splice length of 1.4, should be considered when using Eligehausen's equations to predict a splice length. Table 4.7 has the required splice lengths based on material strengths, however, the capacity reduction factor (ϕ) of ~0.9 is removed from the ACI and AASHTO equations.

Table 4.7 – Required splice lengths based on actual material strengths without the capacity reduction factor (ϕ) of ~0.9.

New Test Series	f_y (ksi)	f'_c (ksi)	τ (ksi)	ACI[1] (in)	AASHTO[2] (in)	Eligehausen[3] (in)
1	60	4.0	1.87	16.6	17.8	12.9

1. Contains a splice length factor of 1.3 for converting development length to splice length.
2. Contains a splice length factor of 1.7 for converting development length to splice length.
3. Contains the recommended splice length factor of 1.4 for converting development length to splice length.

4.8 Chapter Summary

This chapter presents the results from all of the test series. The data was analyzed and examined. The splice lengths were calculated for the ACI and AASHTO equations and the FDOT and Eligehausen adhesive-bonded anchor equations.

CHAPTER 5
SUMMARY, CONCLUSIONS, AND RECOMMENDATIONS

5.1 Summary and Conclusions

The objectives of this project were to:

- Examine the methods used to install adhesive splices and determine if the methods are practical for use on a job site.
- Perform flexural tests to determine the splice length required to achieve full flexural strength when using an adhesive-bonded splice.
- Perform shear tests to determine the shear strength of adhesive-bonded dowel bars.
- Provide design recommendations for splice lengths for adhesive-bonded reinforcement in bridge deck additions.
- Provide design recommendations for determining the shear strength of adhesive-bonded dowel bars in bridge decks additions.

5.1.1 Installation Method

Chapter 3 describes and details the steps taken to drill a hole, clean a hole, and install the anchor using a structural adhesive. The time required for drilling, cleaning, and inserting the adhesive is summarized in Table 5.1. The times in Table 5.1 are the average time each hole took at a given length.

Table 5.1 – Average time of drilling, cleaning, and inserting adhesive for the given embedment depth.

Embedment lengths	20 inches	15 inches	12 inches
Average time to drill	18 min.	9 min.	7 min.

The 20-inch embedment length required removing the drill twice to clean the bit. The 15-inch and 11-inch hole did not require the drill to be removed and cleaned. Based only on time and efficiency it is recommend that the specified embedment length should not exceed 15-18 inches whenever possible.

5.1.2 Flexural Strength

As shown in Table 4.5, the location of the splice bars relative to the existing bars (i.e., the splice bars located in the same plane as the existing bars but either adjacent to or equally spaced between the exiting bars) did not affect the strength of the splice. Therefore, the splice bars can be located anywhere between or next to the existing bars without affecting the strength of the splice.

Test Series 1-3 had failure modes consistent with flexural concrete compressive failure. Test Series 4 failed before reaching a flexural compressive failure. The failure mode observed for Test Series 4 was consistent with a sudden bond failure. As noted in Table 4.6, ACI and AASHTO equations predicted splice lengths greater than the splice lengths used for Test Series 3 and 4. As noted in Section 4.7, Eligehausen's equation, using a capacity reduction factor of 0.9 and the recommended multiplier for splice length factor of 1.4, also predicted splice lengths greater than the splice length for Test Series 3 and 4. Therefore, it is recommended that either the ACI or AASHTO equations for splice length be used without modification. Eligehausen's bonded anchor equations for

adhesive anchor embedment length may also be used with the appropriate modification factors. As mentioned in Chapter 2, Eligehausen's bonded anchor equations are very similar to those in the existing FDOT Design Guidelines with the primary difference being the change in critical spacing from two times the embedment length to sixteen times the anchor diameter. This change should be incorporated in the next revision to the FDOT Design Guidelines.

5.1.3 Shear Strength

All of the shear tests (i.e., Test Series 1-3, Specimen D) performed as expected. The failure mode observed was consistent with the failure mode associated with shear friction. As noted in Section 2.6, the shear strength determined when using shear friction provisions is dependent only on the yield strength of the reinforcement and the coefficient of friction associated with the cold joint between the existing bridge deck and the new bridge deck. As noted in Section 2.6, the coefficient of friction (μ) was taken as 0.60 for concrete placed against hardened concrete that was not intentionally roughened prior to casting the new concrete. Based on a comparison of the test results to those predicted by shear-friction, it is recommended that the shear capacity of adhesive-bonded dowel bars be determined using the shear-friction provisions of either ACI or AASHTO.

5.2 Recommendations for Future Research

It is recommended that an additional test series be performed to verify the use of the ACI and AASHTO splice equations and the 1.4 multiplier for splice length to be used with the adhesive-bonded anchor equations.

The first two test series conducted in this project were adversely impacted by the high compressive strength exhibited by the FDOT Class II concrete for bridge decks (specified strength 3,400 psi, actual strength ~8,000 psi). The splice lengths used in the tests were based on the specified strength of the concrete which resulted in the use of splice lengths in excess of those required when the actual high strength of the FDOT Class II concrete is used in the ACI and AASHTO splice length equations (i.e., the results of Test Series 1 and 2 simply indicated that the splice lengths determined in accordance with ACI and AASHTO did not need to be increased when using adhesive-bonded bars for the splices).

An additional test series with an 18" splice length using concrete with an actual compressive strength of ~4,000 psi, #5 Grade 60 reinforcement, and a minimum end edge distance of eight bar diameters is strongly suggested to provide verification that the ACI and AASHTO splice length equations can be used without modification and the adhesive-bonded anchor equations can be used with the incorporation of a capacity reduction factor of 0.9 and a 1.4 multiplier for splice length.

APPENDIX A - TEST SERIES 1

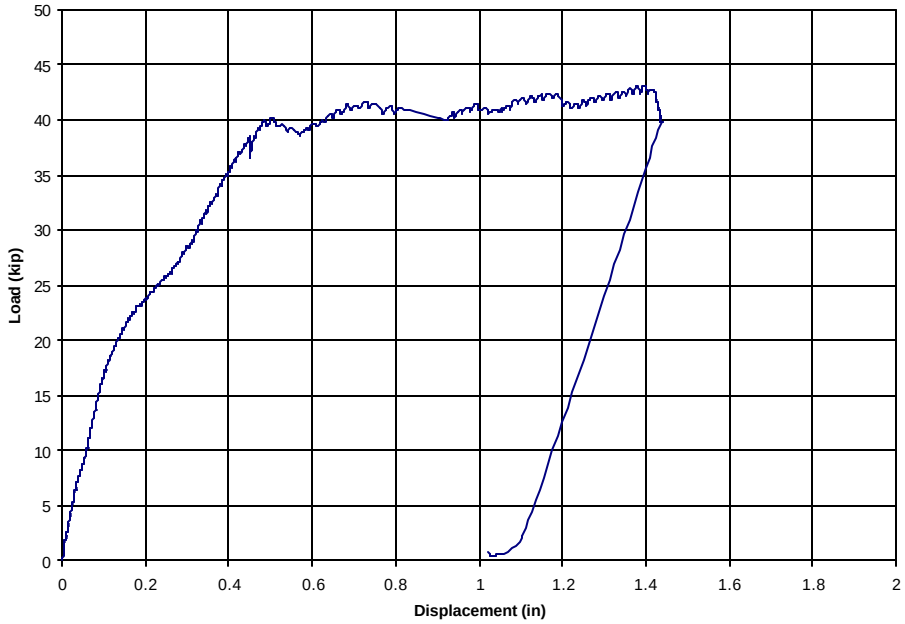

Figure A.1 – Test Series 1 Control Block

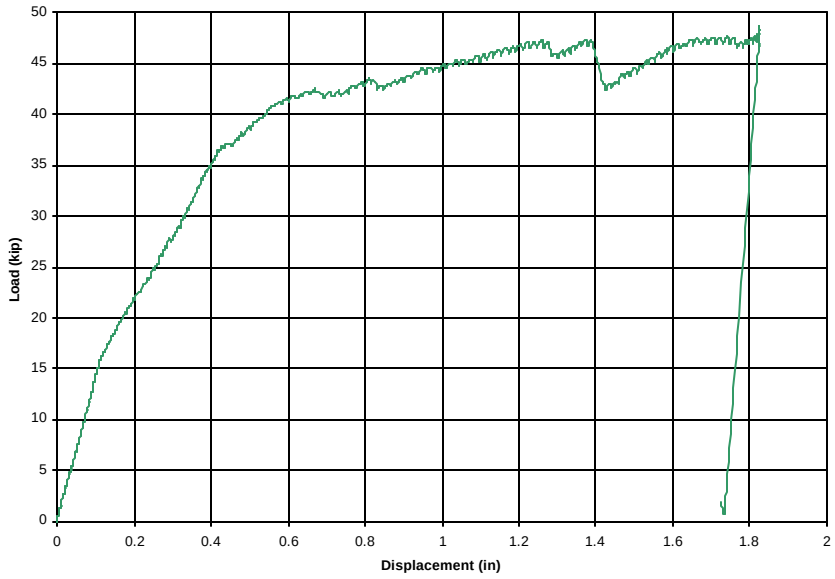

Figure A.2 – Test Series 1, Specimen A

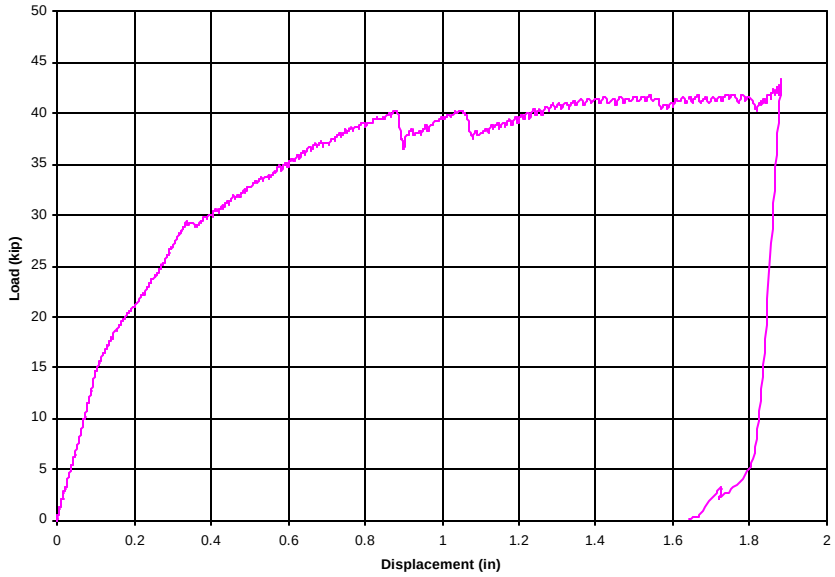

Figure A.3 – Test Series 1, Specimen B

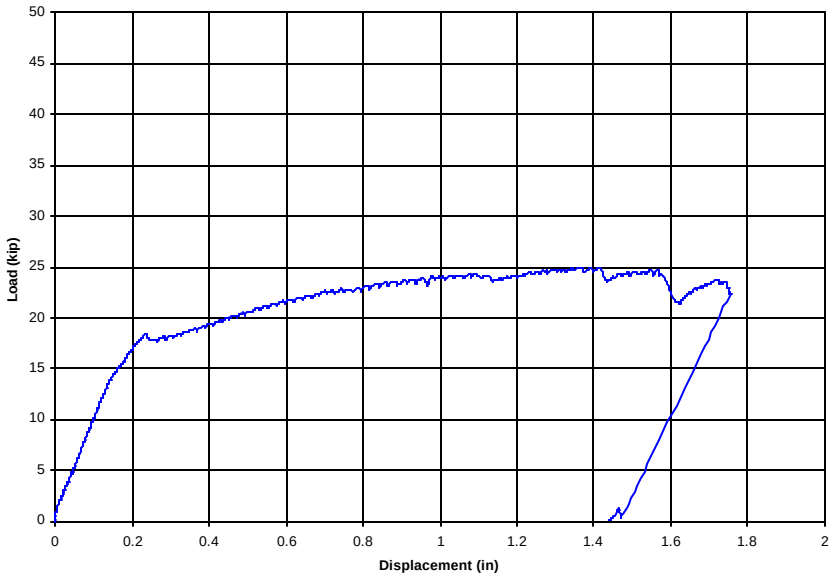

Figure A.4 – Test Series 1, Specimen C

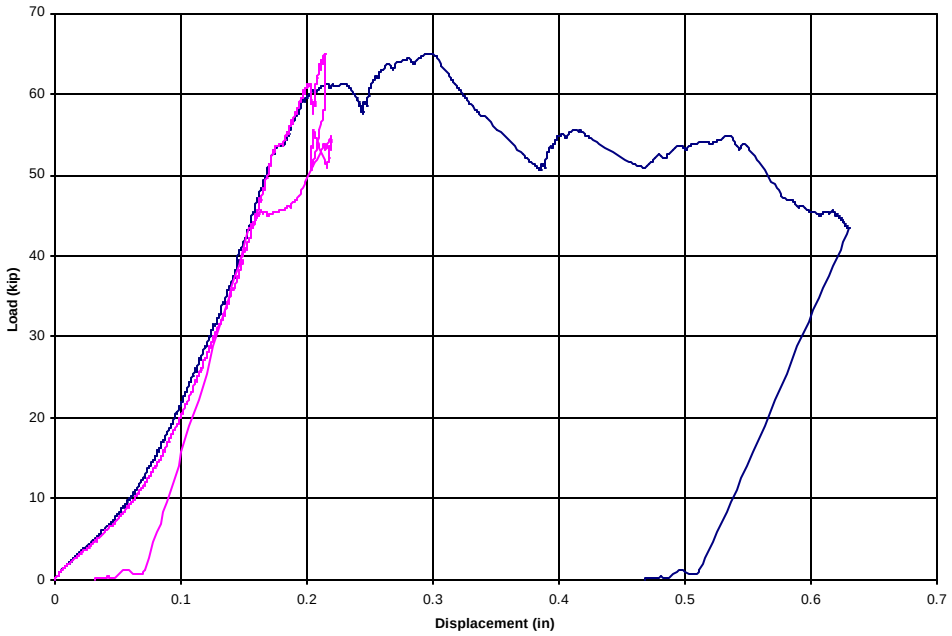

Figure A.5 – Test Series 1, Specimen D

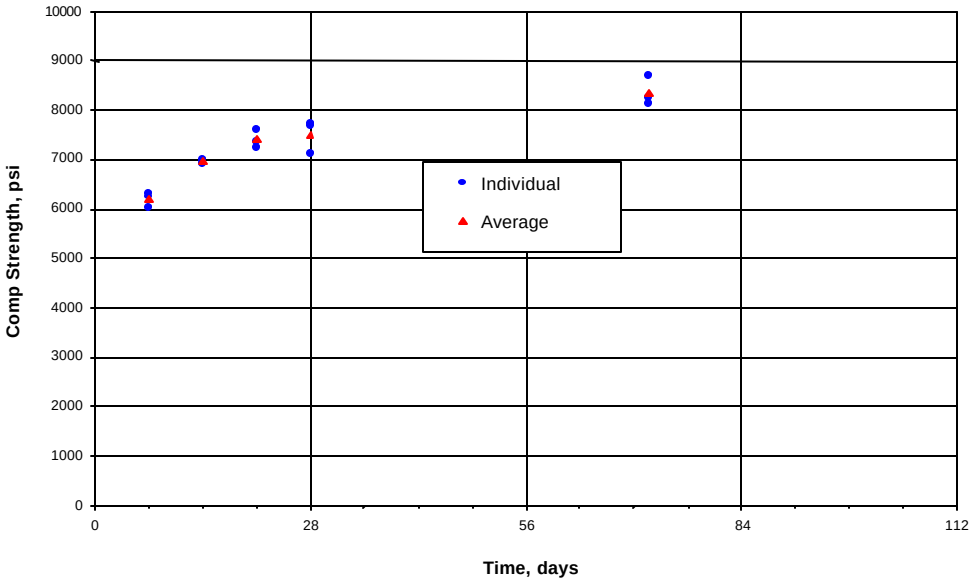

Figure A.6 – Concrete Compressive Strength For Test Specimen 1, Pour 1

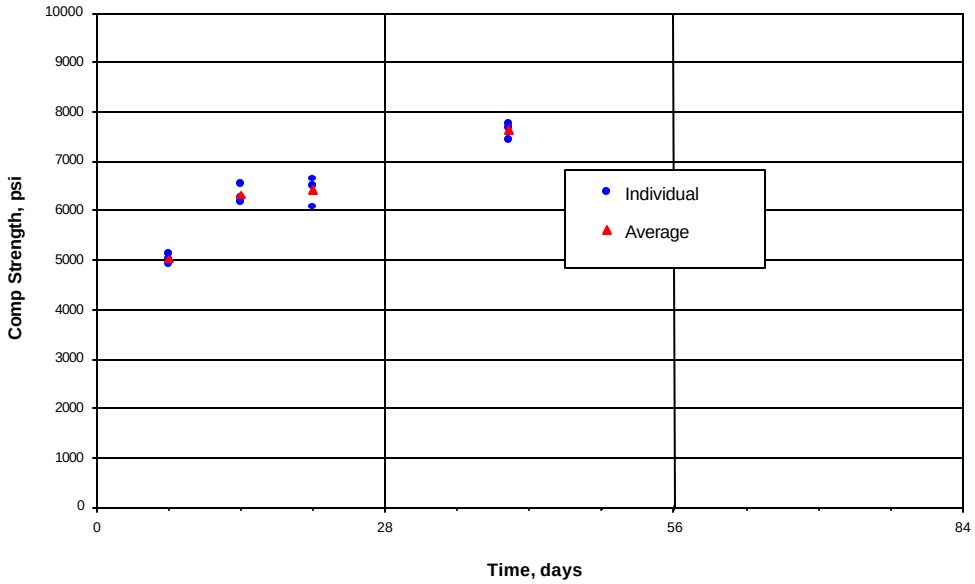

Figure A.7 – Concrete Compressive Strength For Test Specimen 1, Pour 2

Figure A.8 – Test Series 1, Specimen A

Figure A.9 – Test Series 1, Specimen B

Figure A.10 – Test Series 1, Specimen C

Figure A.11 – Test Specimen 1, Specimen D

APPENDIX B - TEST SERIES 2

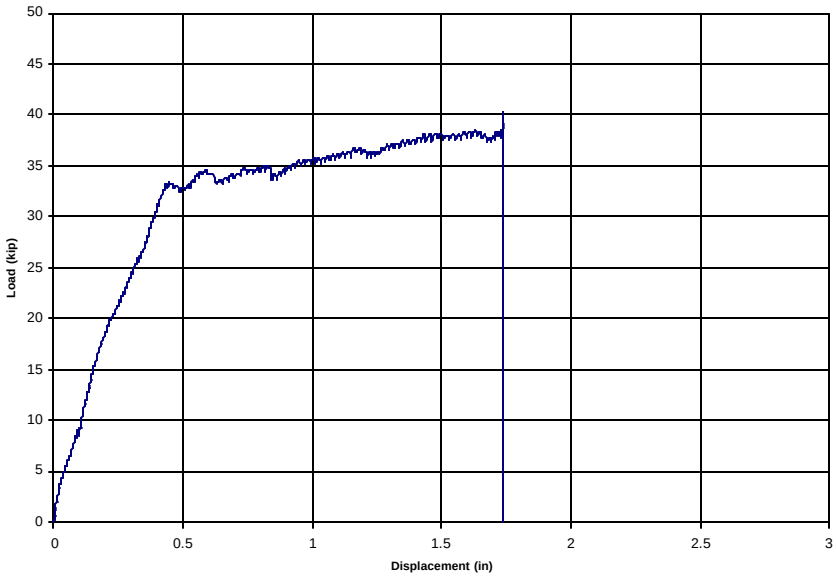

Figure B.1 – Test Series 2 Control Block

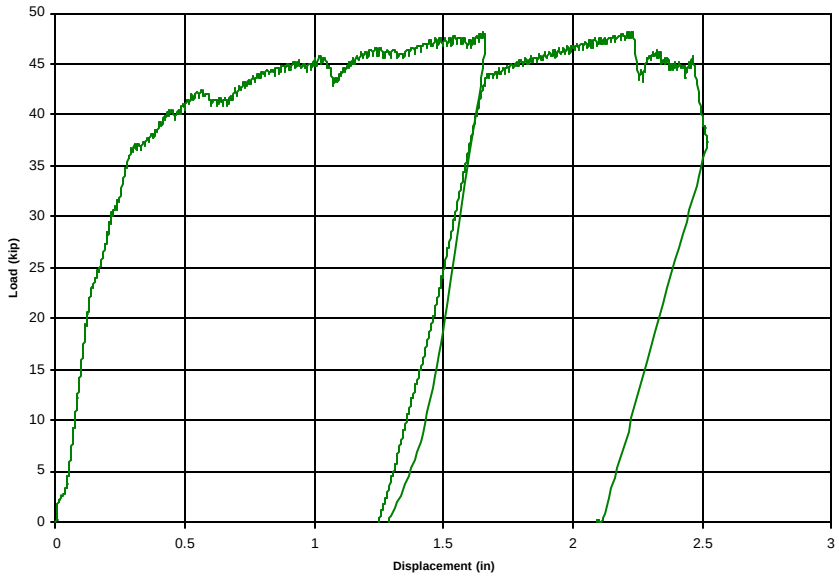

Figure B.2 – Test Series 2, Specimen A

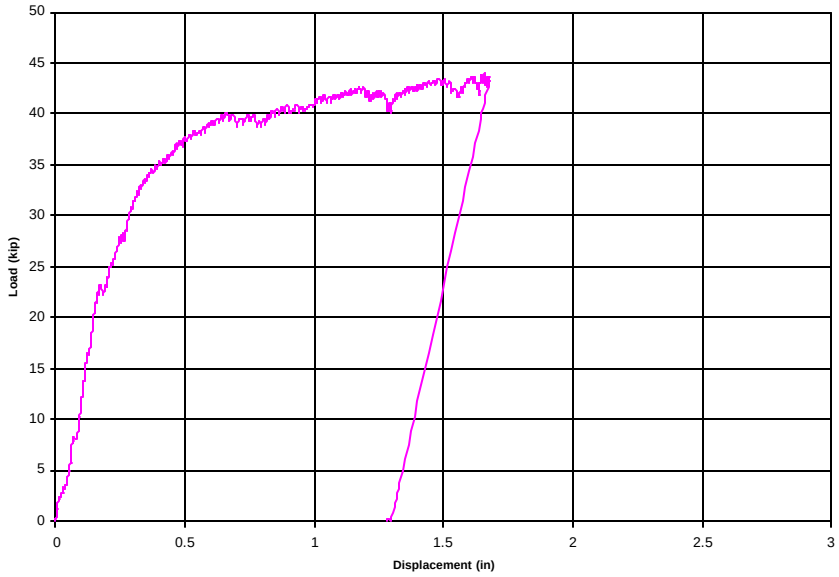

Figure B.3 – Test Series 2, Specimen B

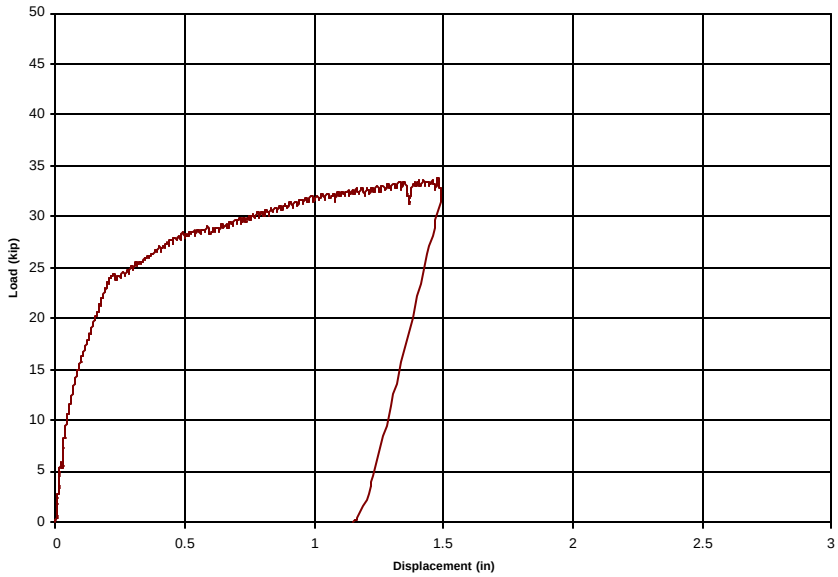

Figure B.4 – Test Series 2, Specimen C

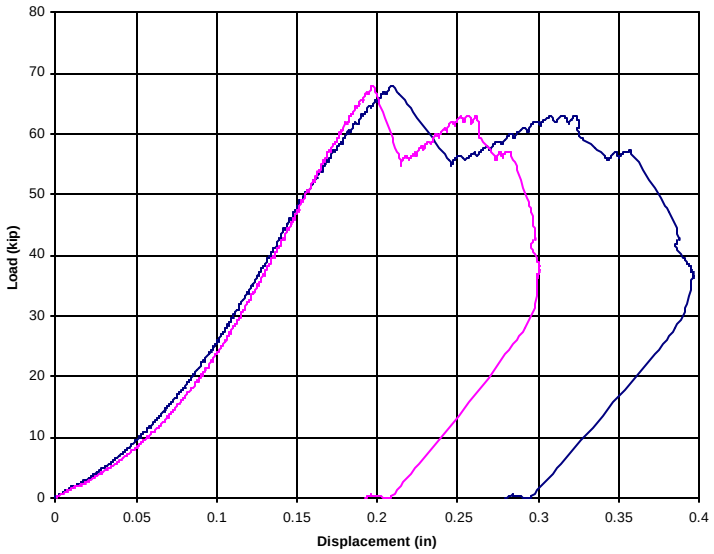

Figure B.5 – Test Series 2, Specimen D

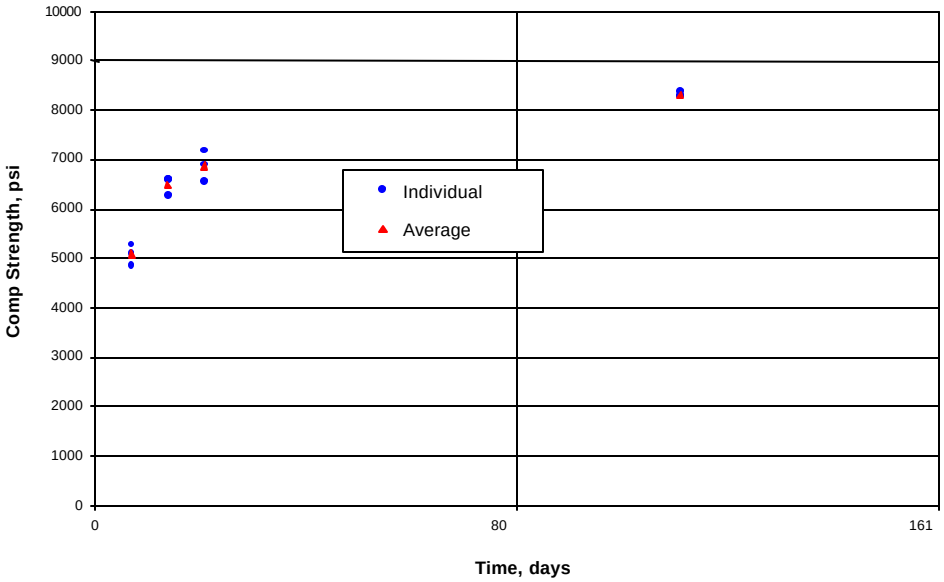

Figure B.6 – Concrete Compressive Strength for Test Series 2, Pour 1

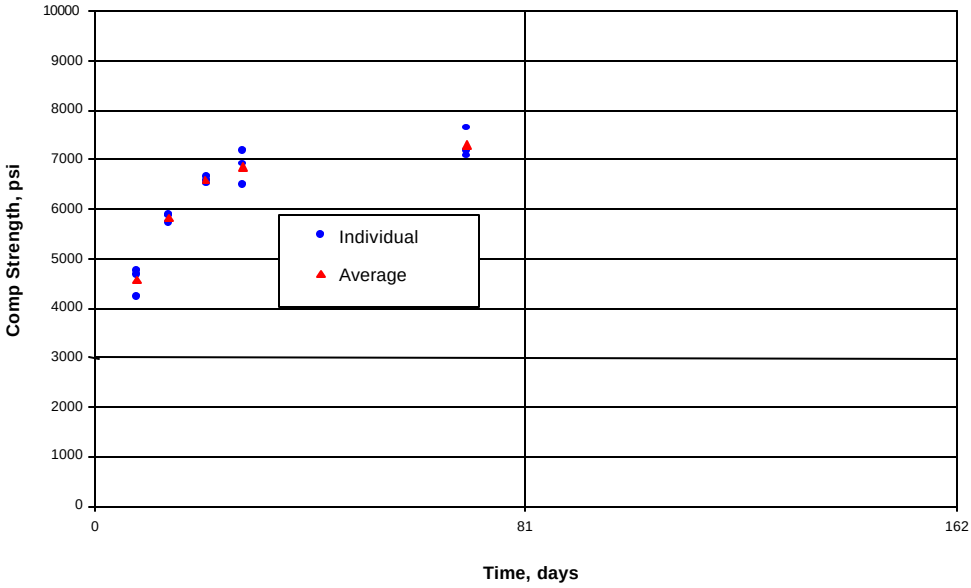

Figure B.7 – Concrete Compressive Strength for Test Series 2, Pour 2

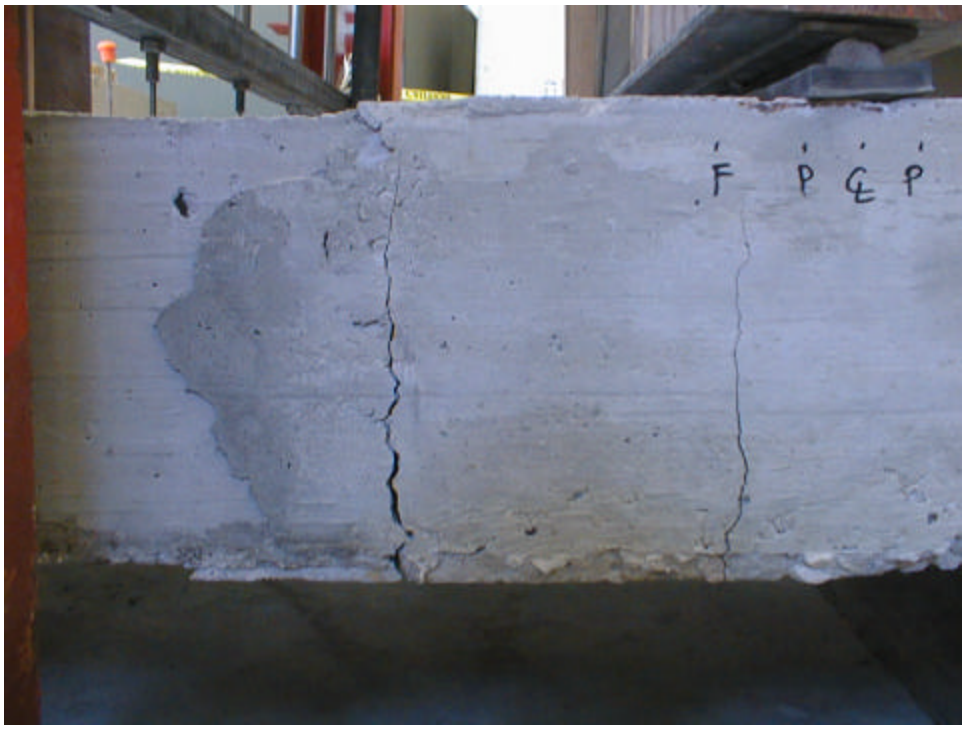

Figure B.8 – Test Series 2, Specimen A

Figure B.9 – Test Series 2, Specimen B

Figure B.10 – Test Series 2, Specimen C

Figure B.11 – Specimen D Splitting failure

APPENDIX C- TEST SERIES 3

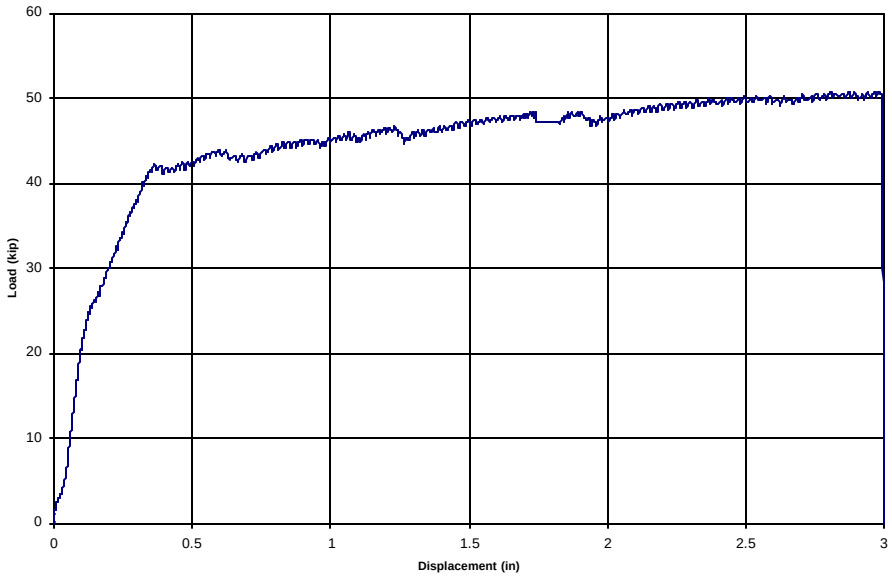

Figure C.1 – Test Series 3, Control Block

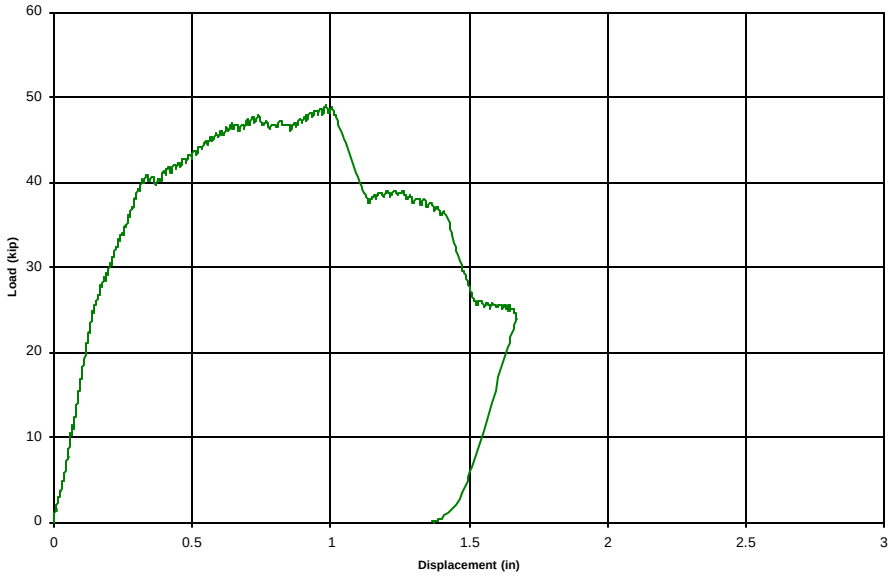

Figure C.2 – Test Series 3, Specimen A

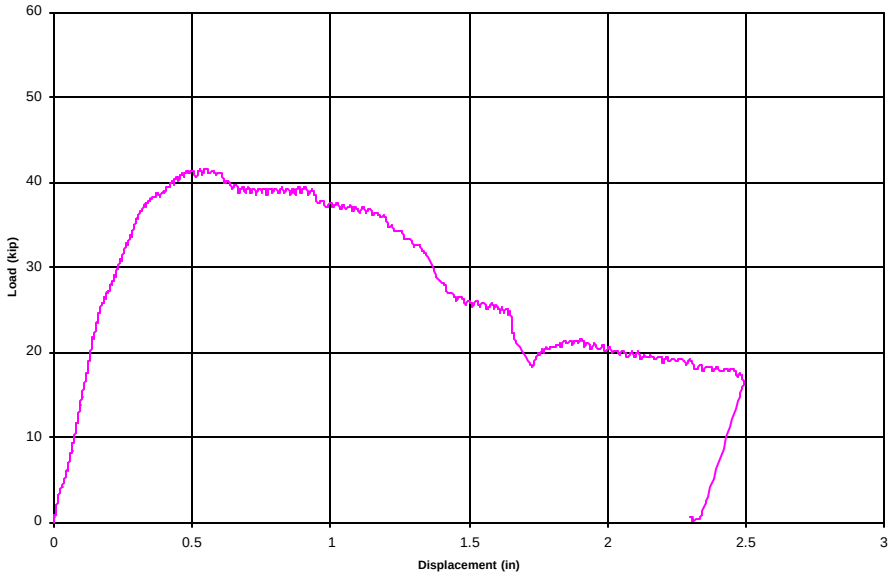

Figure C.3 – Test Series 3, Specimen B

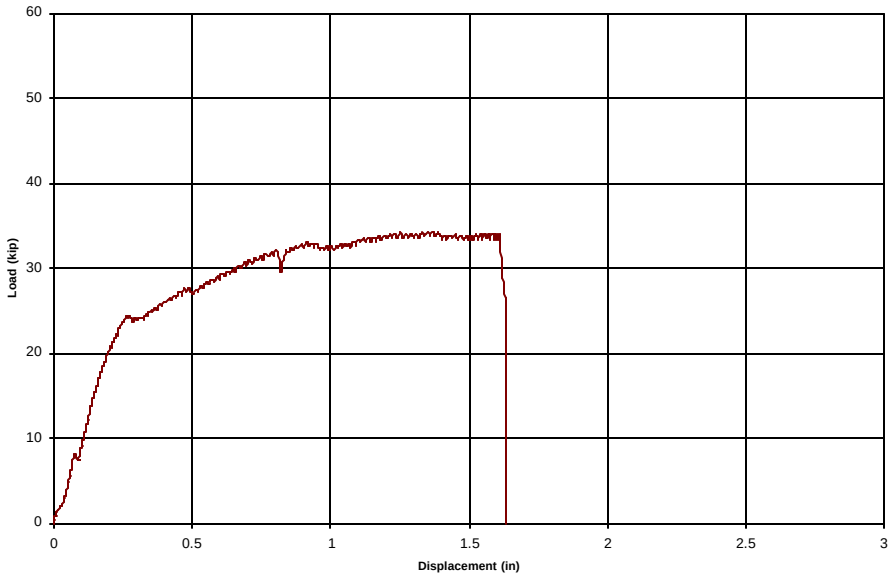

Figure C.4 – Test Series 3, Specimen C

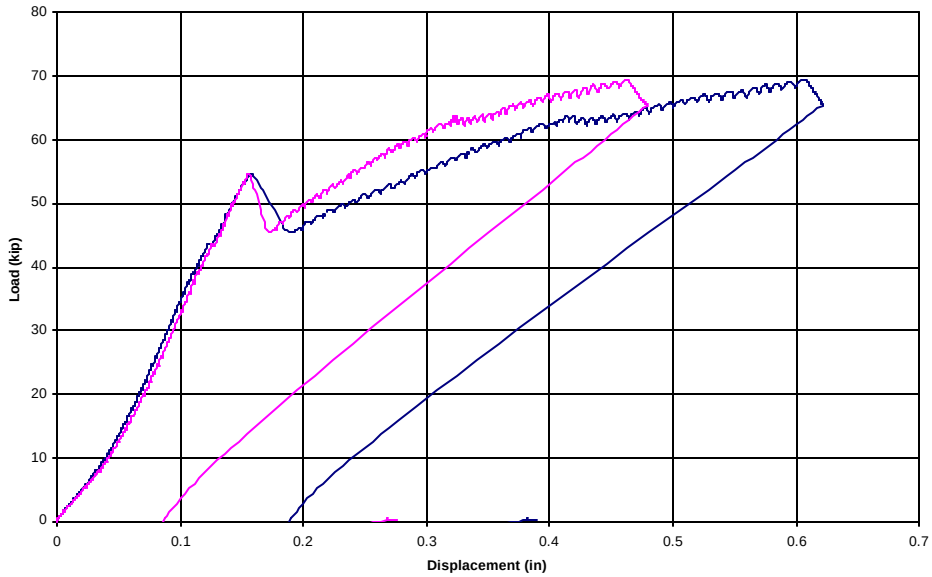

Figure C.5 – Test Series 3, Specimen D

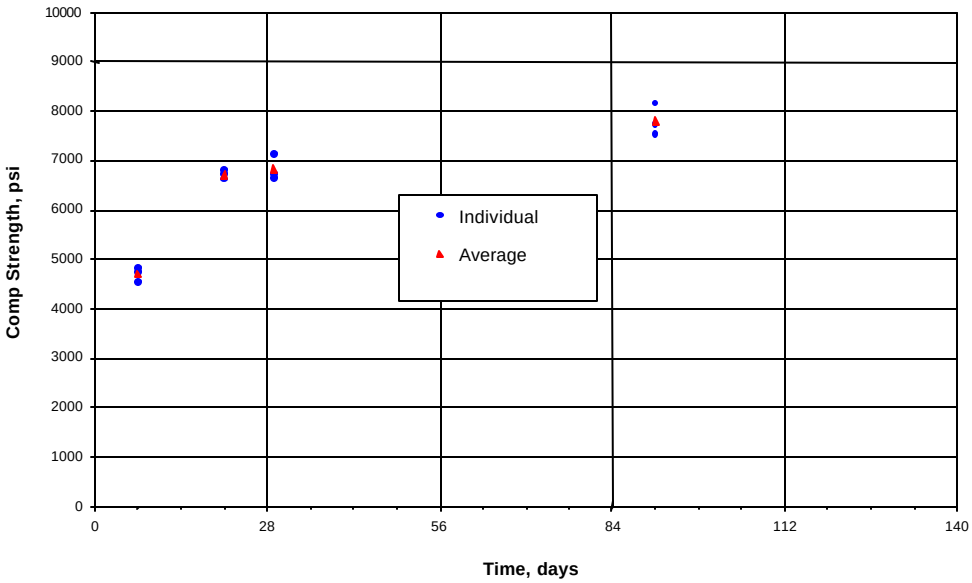

Figure C.6 – Concrete Compressive Strength For Test Series 3, Pour 1

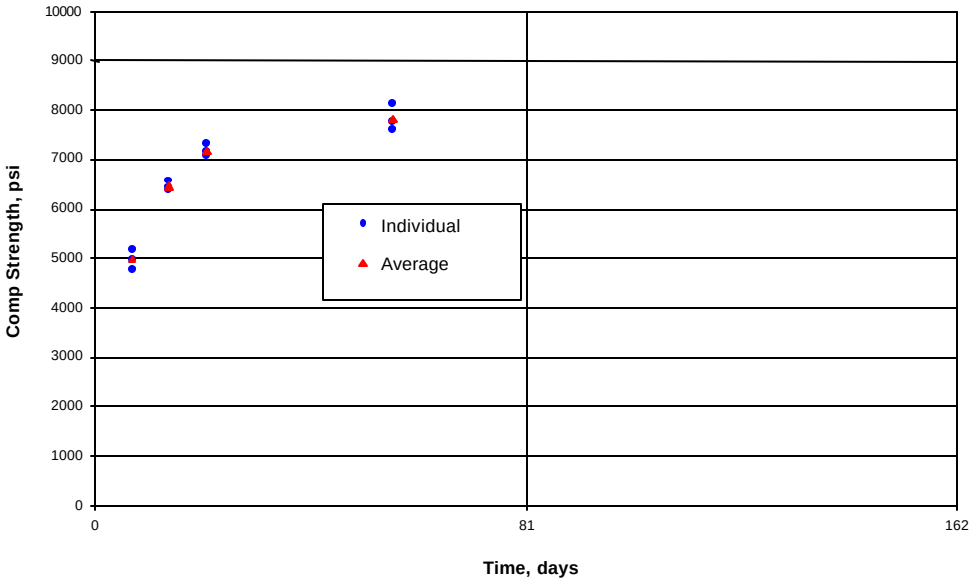

Figure C.7 – Concrete Compressive Strength For Test Series 3, Pour 2

Figure C.8 – Test Series 3, Specimen A

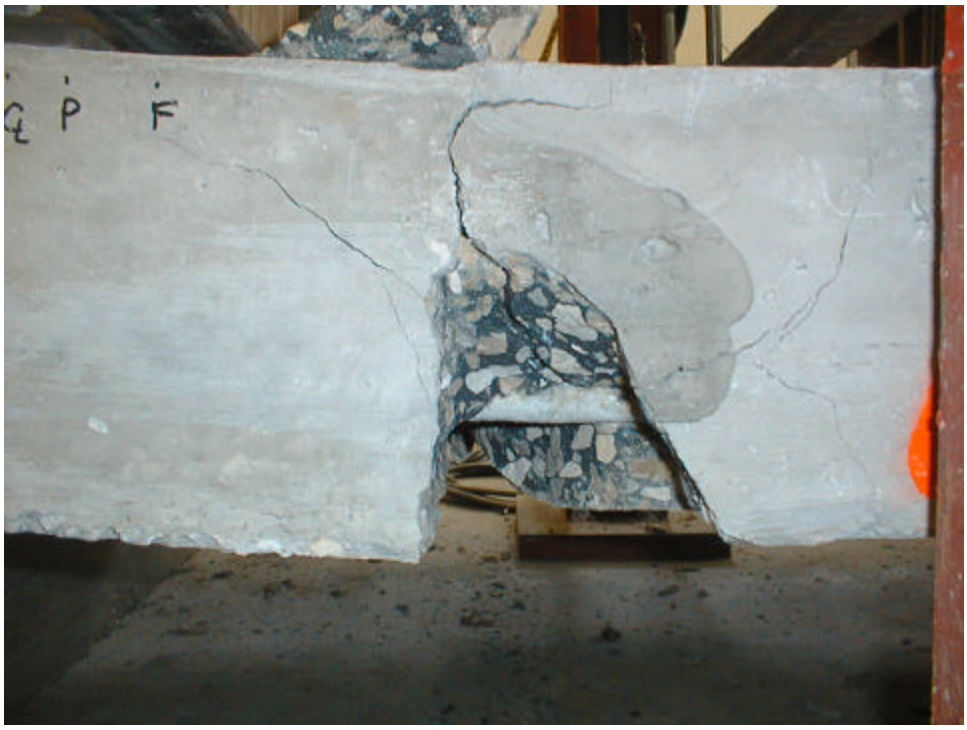

Figure C.9 – Test Series 3, Specimen B

Figure C.10 – Test Series 3, Specimen C

Figure C.11 – Specimen D3 yielding failure

APPENDIX D - TEST SERIES 4

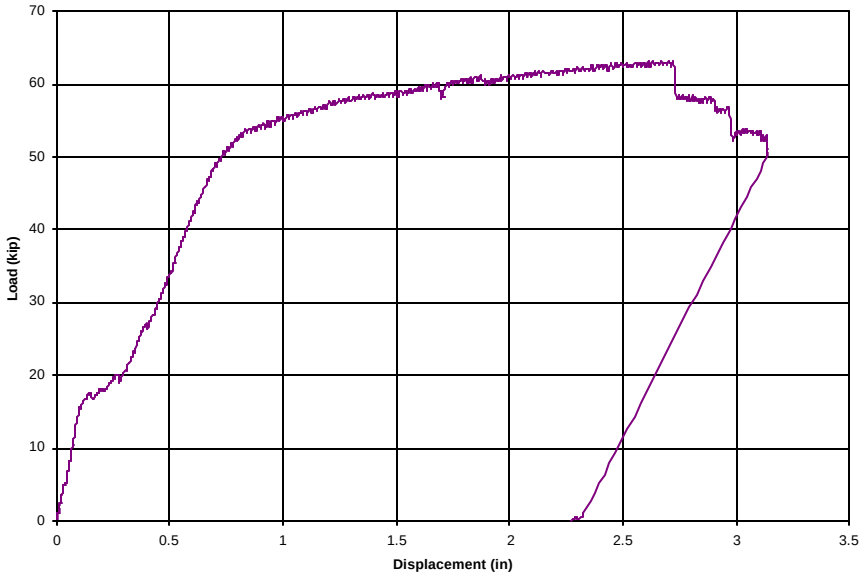

Figure D.1 – Test Series 4, Control Block

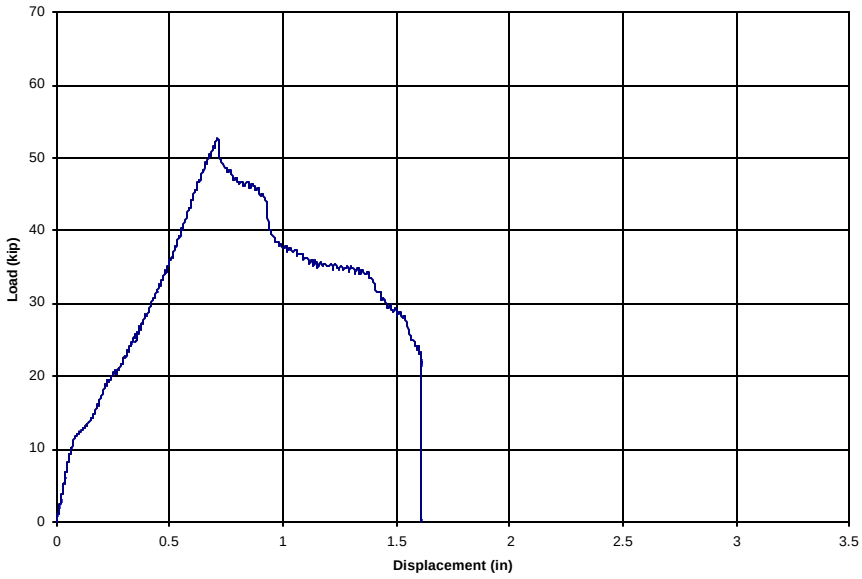

Figure D.2 – Test Series 4, Specimen A

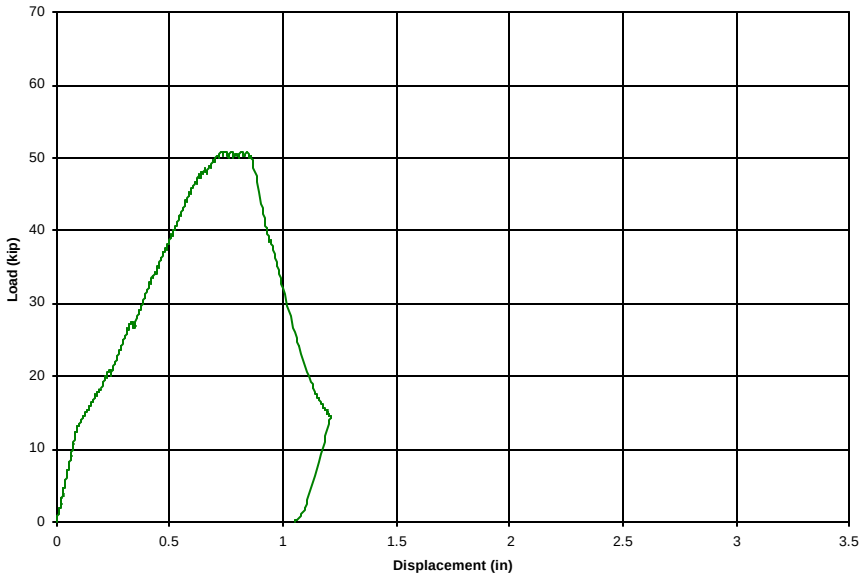

Figure D.3 – Test Series 4, Specimen B

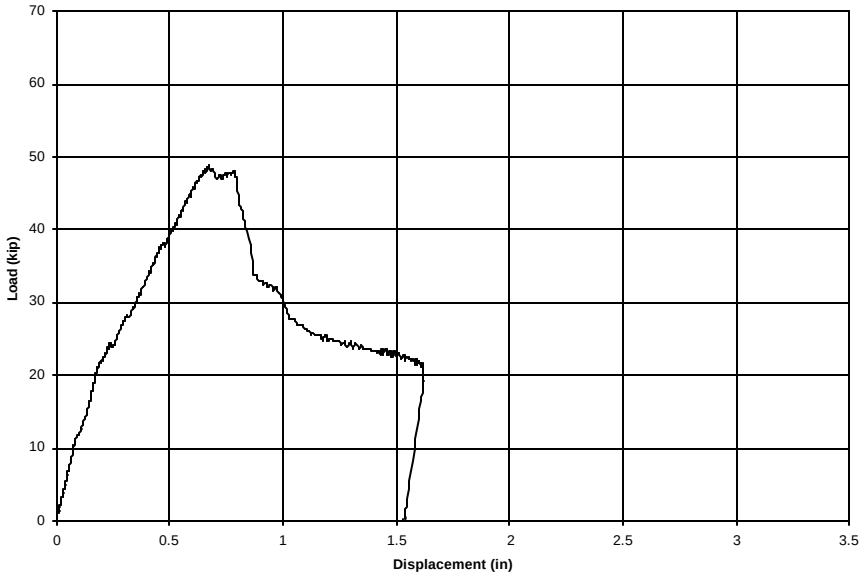

Figure D.4 – Test Series 4, Specimen C

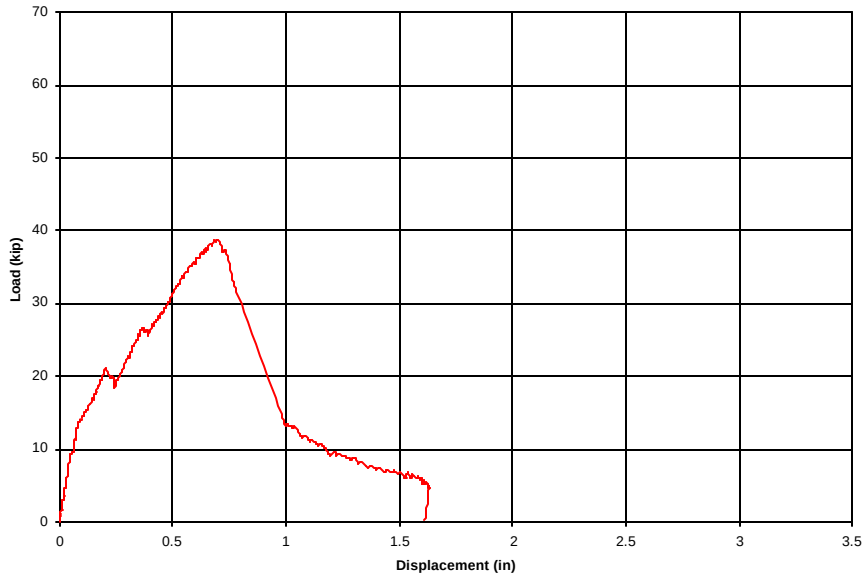

Figure D.5 – Test Series 4, Specimen D

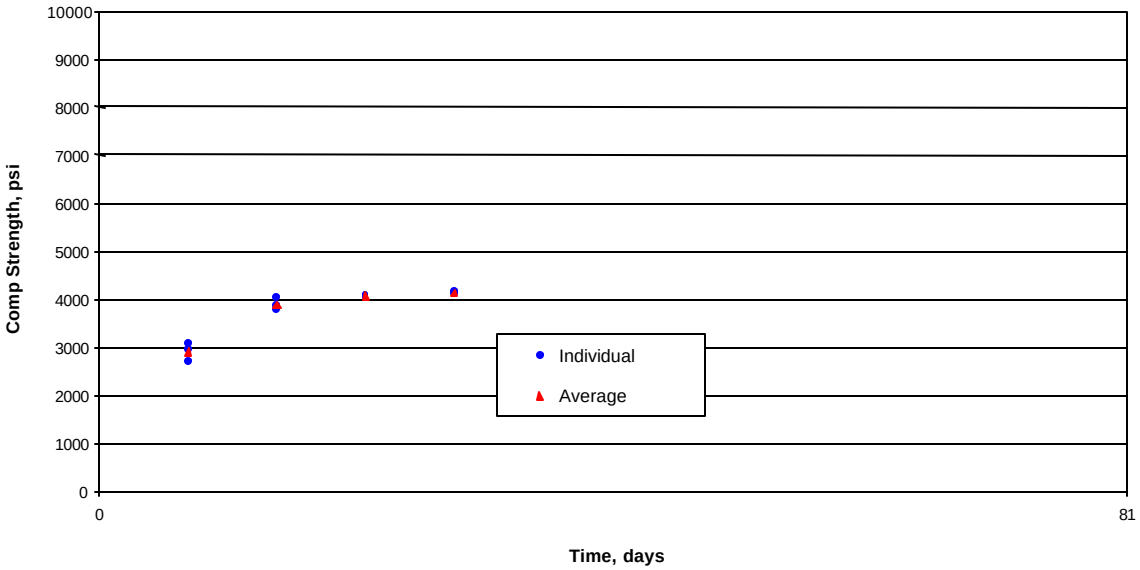

Figure D.6 – Concrete Compressive Strength For Test Series 4, Pour 1

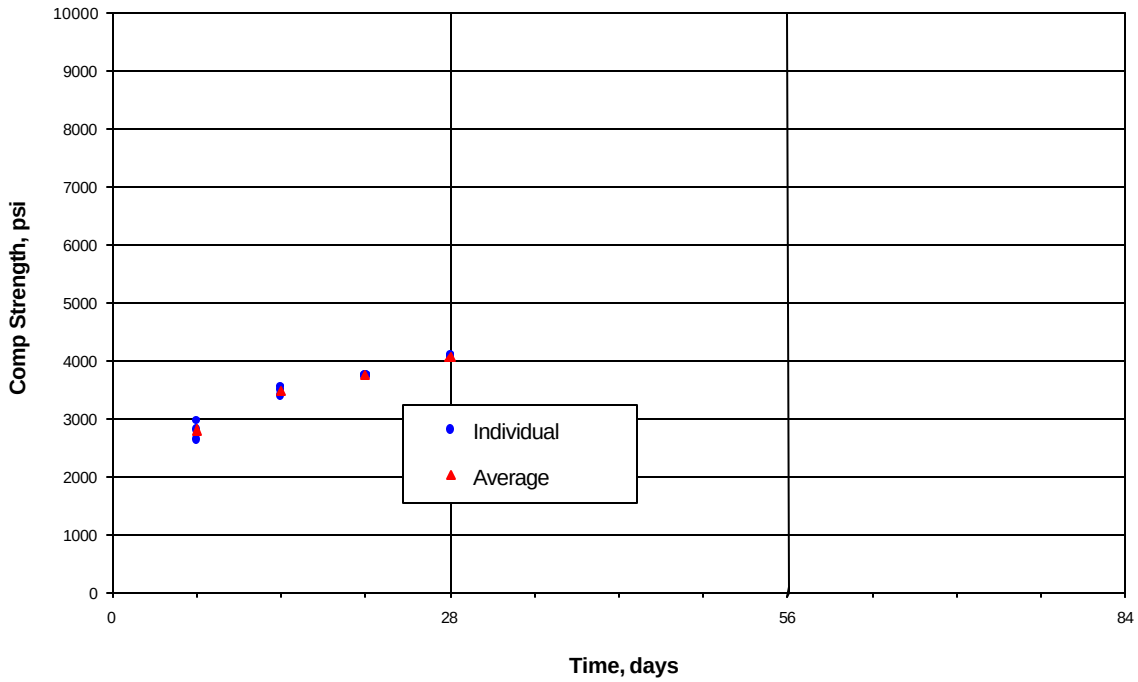

Figure D.7 – Concrete Compressive Strength For Test Series 4, Pour 2

Figure D.8 – Test Series 4, Specimen A

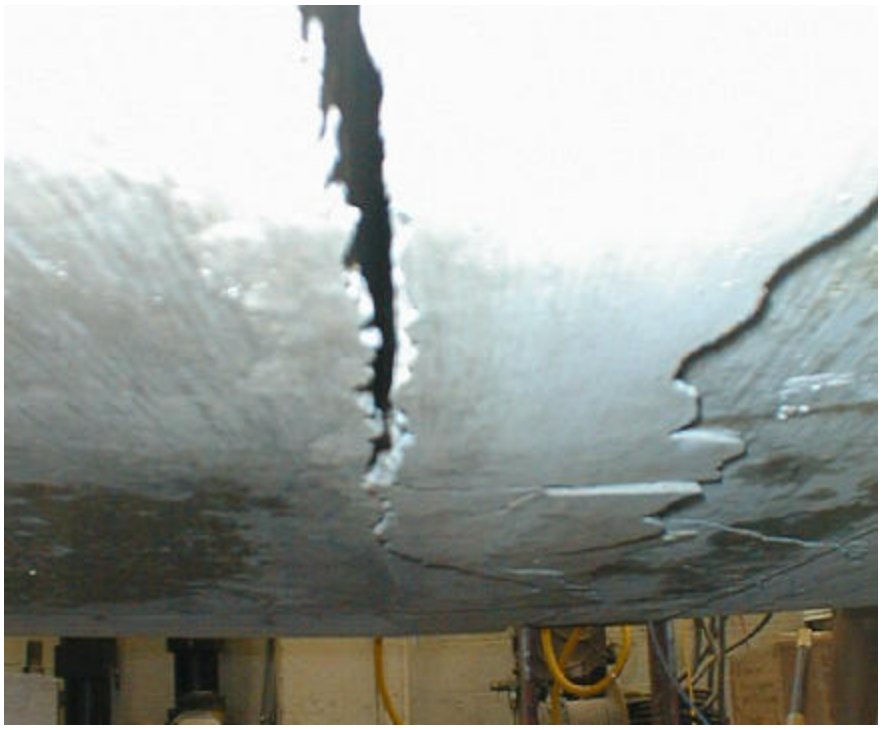

Figure D.9 – Test Series 4, Specimen B

Figure D.10 – Test Series 4, Specimen C

Figure D.11 – Test Series 4, Specimen D

APPENDIX E - TEST COMPARISON

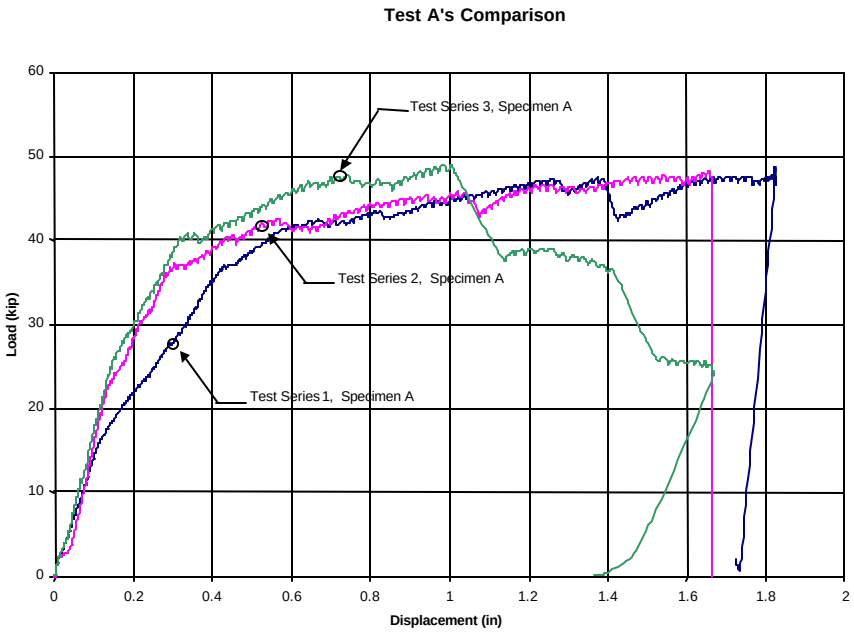

Figure E.1 – Comparison of Specimen A for Test Series 1, 2, and 3

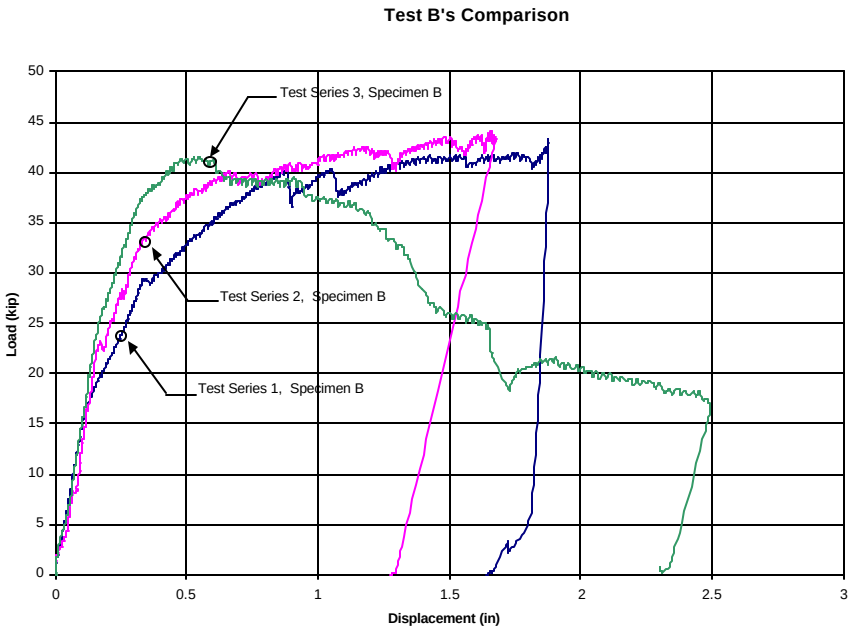

Figure E.2 – Comparison of Specimen B for Test Series 1, 2, and 3

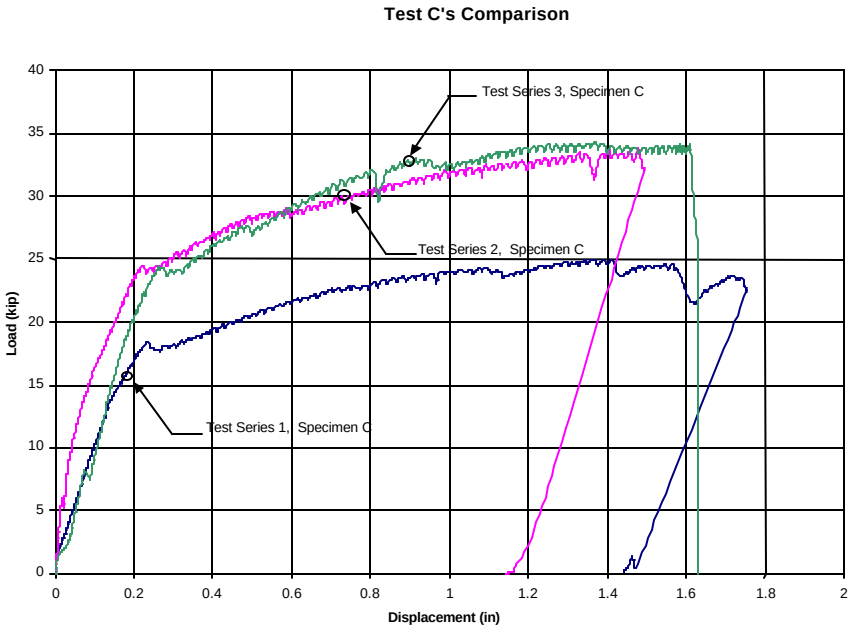

Figure E.3 – Comparison of Specimen C for Test Series 1, 2, and 3

LIST OF REFERENCES

1. AASTHO Highway Sub-Committee on Bridges and Structures, Standard Specifications for Highway Bridges, 1st edition, American Association of State highway and Transportation Officials, Washington D.C., 1994

2. ACI Committee 318, Building Code Requirements for Reinforced Concrete (ACI 318-99) and Commentary (ACI 318R-99). American Concrete Institute, Farmington Hills, MI. 1999.

3. Cook, R. A., Kunz, J., Fuchs, W., and Konz, R., "Behavior and Design of Single Adhesive Anchors Under Tensile Load in Uncracked Concrete," ACI Structural Journal, ACI, V. 95, No. 1, January-February 1998, pp. 9-26.

4. Cook, R. A., and Konz, R., "Factors Influencing the Bond Strength of Adhesive Anchors," ACI Structural Journal, American Concrete Institute, V. 98, No. 1, January-February 2001, pp. 76-86.

5. Florida Department of Transportation,: Structural Design Guidelines, Rev. Jan 1999, pp., 7.9-7.12

6. Lehr, B., and Eligehausen, R., "Design of Anchorages with Bonded Anchors under Tension Load," Proceedings of the International RILEM Symposium on Connections Between Steel and Concrete, Stuttgart, Germany, September 2001, Edited by R. Eligehausen, pp. 411-422.

7. Mains, M.: "Measuring of the Distribution of Tensile and Bond Stresses Along Reinforcing Bars," Journal of American Concrete Institute, V.23, No.3, Nov. 1951. pp., 225-245.

8. McVay, M. C., Cook, R. A., and Krishnamurthy, K., "Pullout Simulation of Post-Installed Chemically-Bonded Anchors," Journal of Structural Engineering, American Society of Civil Engineers (ASCE), V. 122, No. 9, September, 1996, pp. 1016-1024.

9. Rehm, G.: Deutschland,: "Stress Distribution in Reinforcing Bars Embedded in Concrete" Report, pp., 499-505.